

Reviewer #1: We thank you very much for your helpful review. Below are responses to your comments and specific questions.

One problem with TA anomaly when looking at bioerosion is that it measures only the "chemical dissolution". The breaking of CaCO₃ structure is also important and it would have been nice to do buoyant weight measurements to quantify the overall decrease in weight of rubbles (i.e. how much is dissolved vs how much is broken in smaller pieces). This is an important point. Using the TA anomaly method, we can only address the impacts of climate stress on chemical dissolution and not the breakdown of CaCO₃ into smaller pieces (e.g., the production of sponge chips). We have added text to section 2.3 Experimental Design in the revision to clarify this limitation. Note that, because the rubble communities had both secondary calcifiers and bioeroders, the distinction between chemical and mechanical breakdown could not be distinguished using buoyant weight: the change in weight includes both the addition of CaCO₃ by secondary calcifiers and the breakdown of CaCO₃ by eroders. Additionally, it would have been challenging to obtain an accurate estimate of change in buoyant weight given the short duration of the experiment and, therefore, the small magnitude of weight changes relative to the weight of the rubble pieces (1748 g, on average). Nonetheless, we have highlighted this limitation of the TA anomaly method and noted that it is an important distinction for future studies to address.

Specific points:

P12804: What were the flow rates in the mesocosms?

Flow rates were 115 ± 1 (SD) ml min⁻¹, as reported in section 2.4 – Mesocosm Set-up

P12804-I-19: Please provide _ sizes of the rubbles. How was the homogeneity of the rubbles determined? I guess dissolution of old rubbles would be different than the one of "young" rubbles?

There was approximately 1.2L of rubble in each tank, as reported in the third paragraph of section 2.3 – Experimental Design. In response to the reviewer's question, we have added some additional information describing the characteristics of the rubble (3-4 pieces of average weight 499 ± 148 g, average skeletal density of 1.53 ± 0.1 g cm⁻³ (mean \pm SD, n=85)) to give the reader a better sense of the volume and homogeneity of rubble pieces. To keep rubble consistent among aquaria, we kept the volume, weight, and skeletal density of individual rubble pieces consistent and put a similar total volume of rubble in each aquarium. In addition, NEC and NCP rates were normalized to the surface area of rubble in each aquarium. We agree with the reviewer that the age of the rubble could be relevant to the dissolution rate. However, the age of the collected rubble is unknown. We accounted for this in two ways: we controlled for rubble density (expecting that rubble density may be a proxy for rubble age), and we randomized rubble pieces across treatments (so that variation in age adds noise, but not systematic bias, across treatments).

P12804-I-19: Why were the incubations not replicated? 24h incubations are easy to replicates and could have inform on temporal changes.

This manuscript reports the experiment as it was performed. Limitations of facility time and sample cost prevented us from repeating the 24-hour incubations. Despite this limitation, we believe that the results of this experiment give important insights into community calcification processes and will be of interest to Biogeosciences readers.

P12805-I-10: I guess the TA changes in the mesocosms were very limited. Were the errors associated with measurements small enough to be sure to detect a change in calcification? Maybe you should provide the range of TA changes during incubations.

We have added information on the magnitude of TA changes during the day and the night to the methods text in 2.5.1 – Total Alkalinity, the same section where the accuracy and precision of the TA measurements are reported: “The accuracy of the titrator never deviated more than $\pm 0.8\%$ from the standard, and TA measurements were corrected for these deviations. The precision was $3.55\mu\text{Eq}$ (measured as standard deviation of the duplicate water samples). During the 24-hour control experiment, the average changes in TA were $37\mu\text{Eq}$ over the day and $20\mu\text{Eq}$ over the night (day and night TA changes were of larger magnitude in the treatment experiments): these are measurable changes given the precision and accuracy of the TA measurements.” In addition, the regression analysis indicates that the systematic differences due to treatment effects exceeded the variability due to error, including measurement error.

P12808-I-5: What do you mean by normalized to DIN? Do you mean that TA was corrected for the changes in NH_4^+ etc? Please clarify.

TA was corrected for changes in the concentration of nitrate, nitrite, ammonium, and phosphate. We have changed the wording in section 2.6 Measuring Net Ecosystem Calcification and added a citation. It now says “TA was normalized to a constant salinity (35 psu) to account for changes due to evaporation and then corrected for dissolved inorganic nitrogen and phosphate to account for their small contributions to the acid-base system (Wolf-Gladrow et al., 2007).”

P12808-I-11: A change in TA in $\text{mmolCaCO}_3 \text{ m}^{-2} \text{ h}^{-1}$? Reformulate this sentence.

Sentence changed to read, “ F_{TAin} is the rate of TA flowing into an aquarium (= average TA in the header tank times the flow rate), F_{TAout} is the rate of TA flowing out of an aquarium (= average TA in the aquarium times the flow rate), and $\frac{dTA}{dt}$ is the change in TA in an aquarium during the measurement period (change in TA normalized to the volume of water and the surface area of the rubble). The rates are measured in $\text{mmol CaCO}_3 \text{ m}^{-2} \text{ hr}^{-1}$ (specific calculations are given in the supplemental material).”

P12808-I-11: Rates are normalized in $\text{mmol CaCO}_3 \text{ m}^{-2} \text{ h}^{-1}$, does m^{-2} represents the surface of the mesocosms, surface of the rubble, etc? Clarify.

Data are normalized to the surface area of the rubble. This was stated in the original MS on page 12805 line 14 : “... and normalized all our calculations to the surface area of the rubble in each tank”. For clarity, we added “change in TA normalized to the surface area of the rubble” to section 2.6 Measuring Net Ecosystem Calcification and included this detail in the description of the calculations in the appendix.

P12809-I-10: What about the exchanges with the atmosphere? Were the tanks sealed? If not, exchanges with the atmosphere could have lead to under/overestimations of photosynthesis and respiration.

The tanks were not sealed. Air-sea CO_2 flux is minimal for windspeeds less than 10 ms^{-1} (Wanninkhof 1992). In our indoor mesocosm system, the windspeed inside the mesocosm room was near zero. Therefore, we did not account for air-sea fluxes in our analysis.

P12811-I-14: Provide details on the response of NCP.

We have added data on the response of NCP to the results section in the text and in a new table and an extended figure in the main text and in the supplement. Table 3 now includes the regression results for standardized climate change vs NCP, and Figure 3 now has an additional panel showing the relationship between Standardized Climate Change and NCP. Table A2 has the

regression analysis for NCP and Figure A4 shows the means and standard error bars for NCP by treatment.

P12812-I-12: Are the normalization the same? If in the present study the rates are normalized by the actual surface of the rubbles (which needs to be clarified, see above) it might be different than the study of Yates and Halley who normalized by planar surface...

Added this sentence for clarification, "It is important to note that we normalized our rates to the surface area of the rubble while Yates and Halley (2006) normalized their rates to planar surface area." to the discussion.

P12813-I-2-14: I am really not convinced by this explanation for two reasons. – What was the importance of the CCA? Most of the photosynthesis was likely due to turf algae and not to calcify algae. - In addition the authors mention themselves later "non-photosynthesizing invertebrates in the community (such as bivalves) might be dominating the calcification signal in these conditions." In contrast I think that the second hypothesis makes much more sense and should be developed.

We expanded on this point in the discussion. We also added a thermally-induced metabolic response as a possible mechanism. This paragraph now reads as follows:

“1) Some calcifiers can maintain and even increase their calcification rates in acidic conditions (Kamenos et al., 2013; Findlay et al., 2011; Rodolfo-Metalpa et al., 2011; Martin et al., 2013) by either modifying their local pH environment (Hurd et al., 2011) or partitioning their energetic resources towards calcification (Kamenos et al., 2013). For example, in low, stable pH conditions the coralline algae, *Lithothamnion glaciale*, increased its calcification rate relative to a control treatment but, did not concurrently increase its rate of photosynthesis (Kamenos et al., 2013). Kamenos et al (2013) suggest that the up-regulation of calcification may limit photosynthetic efficiency. In the present study, the increase in G_{day} coincided with a decrease in net photosynthesis (Figure 3a,b). Photosynthesizing calcifiers in the community may be partitioning their energetic resources more towards calcification and away from photosynthesis in order to maintain a positive calcification rate (Kamenos et al., 2013). Notably, turf algae likely have a major control over the NCP in this community which would not have any impact on calcification. 2) An alternative hypothesis is that the calcifiers may be adapted or acclimatized to high pCO_2 conditions (Johnson et al., 2014) and have not yet reached their threshold because the rubble was collected from a naturally high and variable pCO_2 environment (Guadayol et al., 2014; Silbiger et al. 2014). 3) In this study, the calcifiers experienced a combined increase in both pCO_2 and temperature and, thus, the non-linear response in G_{day} may also be due a metabolic response. In a typical thermal performance curve, organisms increase their metabolism until they have reached a thermal maximum and then rapidly decline (Huey and Kingsolver, 1989; Pörtner et al., 2006), and we see this response in our results. A recent study found a similar nonlinear response to temperature and pCO_2 in the coral *Siderastrea sidera* (Castillo et al. 2014). While they attribute the pCO_2 response to photosynthesis being neutralized (we did not see this response in our non-coral community), they suggest that the thermal response is due to both changes in metabolism and thermally-driven changes in aragonite saturation state (Castillo et al. 2014).”

-P12814-I-7-15: I agree with this paragraph but it would be important to specify that this is true for an ecosystem dominated by rubbles. In an ecosystems with very high coral cover, the story would likely not be the same...

We clarified that this generalization is specific to our rubble community. This sentence now reads, “Standardized Climate Change explained more of the variance in dissolution than

in calcification in our rubble community: ($R_{G_{night}}^2 = 0.64 > R_{G_{day}}^2 = 0.33$; Table 2) this result is not surprising”

Reviewer 2: We thank you very much for your helpful review. Below are responses to your comments and specific questions.

General comments:

As a more general question though I wondered the following: since the organisms being studied here are described as “secondary calcifiers” how do their responses impact coral reefs directly, which I’m assuming is thought of in this context as “primary calcification”?

While secondary calcification contributes significantly less to the overall growth of coral reefs than primary calcifiers (such as corals), secondary calcifiers still play several key ecological roles on coral reef ecosystems. For example, they help to cement the reef together which maintains reef stability, and they produce chemical cues that induce the settlement of many types of invertebrate larvae (including corals). I have added this information to the introduction.

Specific points:

1. (12802, 20) – Is it “increase to 557 ppm by the year 2100” (rather than “increase by 557 ppm the year 2100”)?

The increase actually is "by 557", not "to". RCP 8.5 is a high-emissions scenario, but one that we are currently tracking. Meinshausen et al., 2011 states that under the RCP8.5/ECP8.5 scenario pCO₂ is predicted to be 936ppm by 2100, which is 557ppm above current levels (379ppm).

2. (12804, 9) – How long were the aquaria monitored without rubble to establish the stability conditions in Table 1? How many measurements were made to determine the mean values in this table?

The data presented in Table 1 are from one 24 hour cycle: each aquarium was measured in the light and then, again, in the dark. Each entry in the table is the average of 12 measurements: day samples and night samples for each of the six aquaria. This is now clarified in the text and the table caption. We have also changed the wording to reflect that these measurements demonstrate the consistency of the treatments within each rack between day and night, but not temporal stability, persay. The temporal stability of the mesocosm system was measured over a 26 day period and is reported in Putnam (2012). We have added this citation to the ms.

3. (12807, 2) - Is there a reference for the technique used to determine pH?

Yes, the reference is Dickson, A. G., Sabine, C. L., and Christian, J. R.: Guide to best practices for ocean CO₂ measurements, 2007. This was referenced later in the paragraph, but we have added it to the end of line 3 for clarity.

4. (12808, 5) – I think there must be some words missing here in this description of how things were normalized to DIN.

This sentence now reads, "TA was normalized to a constant salinity (35 psu) to account for changes due to evaporation and then corrected for dissolved inorganic nitrogen and phosphate to account for their small contributions to the acid-base system (Wolf-Gladrow et al., 2007)."

5. (Eqn. 1) - I think a little more detail is needed for how the 3 measurements made per experiment (12805, 7-11) were specifically used in this equation (i.e., which values were used to determine the F values, and which were used for dTA/dt). The same is true for Eqn. 2 although I assume the same general approach was used in both cases.

We added some additional text to describe the equation. “ F_{TAin} is the rate of TA flowing into an aquarium (= average TA in the header tank times the flow rate), F_{TAout} is the rate of TA flowing out of an aquarium (= average TA in the aquarium times the flow rate), and, $\frac{dT_A}{dt}$ is the change in TA in an aquarium during the measurement period (change in TA normalized to the volume of water and the surface area of the rubble). The rates are measured in $\text{mmol CaCO}_3 \text{ m}^{-2} \text{ hr}^{-1}$ (specific calculations are given in the supplemental material).”

Additionally, we added the specific calculation for F_{TAin} , F_{TAout} , and $\frac{dT_A}{dt}$ to the supplemental files. These calculations follow Andersson et al. 2009, as referenced in the text.

6. (12810, 5) – I’m not sure I understand why a simple product of temperature and pCO₂ was used as the independent variable (i.e., the one sentence explanation here seems inadequate to me).

We agree with the reviewer that a simple product of pCO₂ and temperature was not straightforward to interpret. We have revised the manuscript so that the Standardized Climate Change (SCC) axis is a simple linear combination of $\Delta p\text{CO}_2$ and $\Delta \text{Temperature}$ that puts $\Delta p\text{CO}_2$ and $\Delta \text{Temperature}$ on the same scale. The results and interpretations of our study are the same with this new axis (indeed, any of several choices of synthetic axes produced similar results). Further, we added figures to the supplement showing G and NCP versus $\Delta p\text{CO}_2$ and versus $\Delta \text{Temperature}$ to show that the relationships between G and NCP versus $\Delta p\text{CO}_2$ and $\Delta \text{Temperature}$ are similar to the relationships using the combined axis (Standardized Climate Change). Here is the explanation of our new version of the SCC axis in the text:

“Although we imposed four discrete temperature-pCO₂ scenario treatments on each tank (Table 1), random variation between treatments and the feedback between the rubble communities and the water chemistry resulted in near-continuous variation in temperature-pCO₂ treatments across aquaria (Figures 2 and A1). To capture this continuous variation in temperature-pCO₂ in the analysis, we used the measured temperature-pCO₂ seawater condition as a continuous independent variable in a regression rather than the four categorical treatment conditions in an ANOVA (an analysis of G and NCP using the ANOVA approach is included in Figures A3, A4 and Tables A1, A2). The regression approach allowed us to better capture the quantitative relationships between net calcification (G) or NCP and the temperature-pCO₂ treatment. We created a single, continuous variable, Standardized Climate Change (SCC), from a linear combination of temperature and pCO₂ values in each aquarium. A simple linear combination was used because pCO₂ increased linearly with temperature (Figure 2), as imposed by our treatments. We first calculated the relationship between ΔTemp (Eq 3) and $\Delta p\text{CO}_2$ (Eq 4) using linear regression. The coefficients from this regression (slope: $\alpha = 0.0031$; y-intercept: $\beta = -0.078$) were used to combine pCO₂ and temperature onto the same scale, as a measure of Standardized Climate Change (Eq 5):

$$\Delta \text{Temp}_i = \text{Temp}_{trt,i} - \text{Temp}_{cont,i} \quad \text{Eq. 3}$$

$$\Delta p\text{CO}_{2i} = p\text{CO}_{2trt,i} - p\text{CO}_{2cont,i} \quad \text{Eq. 4}$$

$$\text{SCC}_i = \Delta \text{Temp}_i + \alpha * \Delta p\text{CO}_{2i} + \beta \quad \text{Eq. 5}$$

This synthetic temperature-pCO₂ axis, SCC, is centered on the ambient (control) conditions such that a value of 0 corresponds to present day Kāne‘ohe Bay conditions, a negative value corresponds to water that is colder and less acidic (pre-industrial) and a positive value corresponds to water that is warmer and more acidic (future conditions) compared to background seawater. (The independent relationships between G and NCP with ΔTemp and $\Delta p\text{CO}_2$ are shown in Figures A5 and A6 and are similar to the relationship with SCC.)’

7. *It also occurred to me that if calcification rates vary differently in response to changes in temperature versus changes in pCO₂, then this might explain the non linear response seen in Fig. 3A. I would think that this might be considered a bit more explicitly in the discussion starting on line 24, p. 12812.*

Yes, we agree. We have added a section to the discussion about the impact of temperature on daytime calcification, specifically focusing on metabolic response.

8. *(12811,15) – Which G values were used in Figs. 4 and 3A? Since $G_{net} = G_{day} + G_{night}$, using G_{net} here (along with G_{day} and G_{night}) would seem to be “double dipping” with the data.*

G_{net} is the sum of G_{day} and G_{night} . We thought that it was critical to show our readership the response of net calcification over a 24 hour cycle. Figure 3e highlights the aquaria that were net calcifying or net dissolving over the entire experiment. It is difficult to elucidate this from figures 3a and c alone. We added a line at the zero point in 3e to further highlight that there is a shift from net calcification to net dissolution over the 24 hour cycle. The data shown in Figure 4 are simply the day (squares) and night (circles) data. The figure legend reads: "Squares are data collected during the light (day) conditions and circles represent data collected during dark (night) conditions".

“Double dipping” typically refers to an iterative analysis where initial analyses or preprocessing of data guides subsequent analyses and increases the likelihood that the subsequent analyses are significant. Here, the separate and planned analyses of day, night, and net are critical because each analysis gives distinct information to the reader about the community response to climate change when (day) photosynthesizers are active and (night) when all members of the community are respiring, and (net) whether there is net calcification or net erosion over a diel cycle. Although G_{net} is not statistically independent of G_{night} and G_{day} , it is still appropriate to analyze the sum separately from the components: for example, consider if G_{day} had a positive relationship with SCC and G_{night} had a negative relationship with SCC and, when summed, G_{net} had no significant relationship with SCC. Each of these results would tell us something different and important about the relationship between calcification and SCC (daytime calcification increases with SCC, nighttime calcification decreases with SCC, and daily net calcification is unaffected by SCC). Although the actual results of this study are somewhat more complex, all three analyses must be presented for the reader to understand the dynamics of the system.

9. *(12811, 21) – Maybe I’m getting caught up in semantics but referring to changes in carbonate system parameters due to calcification, dissolution, photosynthesis and respiration as “feedbacks” seems to imply a bit more complexity than is really occurring. I’m not sure I would use this word here and throughout the manuscript to describe how these biological processes affect carbonate chemistry.*

We disagree. As CO₂ is added to the water it impacts the biology of the organisms, and those biological responses then also change the water chemistry. For example, increased pCO₂ decreases pH which may result in increased erosion/dissolution, or increased pCO₂ may enhance photosynthesis, which could increase erosion/dissolution by autotrophic microborers (Tribollet et al. 2009). The enhanced photosynthesis then also alters the seawater chemistry. This interaction between the biology and chemistry causes a feedback loop. The term "Feedbacks" has been used in the literature (e.g., Jury et al 2011, Anthony et al 2011) to describe the interaction between increased CO₂ from the atmosphere and biological responses (e.g. calcification, dissolution, respiration, and photosynthesis) in altering the chemistry of the seawater. In our study, we saw a positive relationship between the amount of CO₂ that we added to the mesocosms and the deviation in CO₂ from the intended concentration (Figure A1). If there were no feedbacks, then the relationship between pCO₂ with rubble and pCO₂ without rubble from each aquarium would

have a slope of one with a fixed offset (change in y-intercept) due to increased respiration by the organisms. With feedbacks, we would expect that as pCO₂ increases, feedbacks would increase resulting in deviations from the 1:1 slope. During the day, we saw a slope of 1.1 while during the night, the slope was much greater than one (slope = 1.4, Figure A1b). This relationship suggests that there were feedbacks in our mesocosms. We added regression lines to Figure A1 to better illustrate these feedbacks.

10. (12811,17) - I think it would help if the data described here as “exceptions” were explicitly indicated on Figs. 4 and 3A (perhaps circled on the figure?). This concern is also relevant to discussions on p. 12813, line 24 [‘This hypothesis . . .].)

We have changed the text to explicitly call out the points in the upper left quadrant with the points in the upper right and lower left quadrants of Figure 4. We have also added $y = 0$ lines to Figure 3 to make it easier for the reader to identify the net positive versus net negative values. We have shied away from circling these specific points on the graph so as not to distract readers from their own interpretations of patterns in the data. However, we have called out these points much more descriptively and specifically in the text to help orient the reader to the plots – thank you for highlighting the need for this direction.

11. *In section 4.2, please don't switch flux units. Mixing 'per day' flux units with 'per hour' flux units makes it very difficult on the reader. If necessary, convert data from the literature to the units you wish to use in the manuscript.*

We switched the units to $\text{mmol m}^{-2} \text{d}^{-1}$ in the text.

12. (12813,10) – *“In the present study . . .”. Where is this shown? Is “net photosynthesis” actually NCP?*

We added a panel with the NCP data to figure 3 and associated references, in the text; we also changed “photosynthesis” to “NCP”.

13. (12813,18) – *‘We saw a decline . . .’. Again, where is this shown?*

We added a citation to Figure 3 after this sentence.

14. (12814, 7) – *How exactly is “strongly affected” defined here?*

We changed the wording to be more precise: “Standardized Climate Change explained more of the variance in dissolution than in calcification in our rubble community: ($R_{G_{night}}^2 = 0.64 > R_{G_{day}}^2 = 0.33$; Table 2) this result is not surprising”

15. (12814, 15) – *Talking about “distinct” responses here seems a little vague.*

We added “: G_{day} had a non-linear response while G_{night} declined linearly with Standardized Climate change” for clarification.

16. *Figure 4 – Why is the color scale for standardized climate change multiplied by 10^4 ?*

This has been corrected in the revised manuscript using the new Standardized Climate Change axis.

17. *Figure A3 – Is the y-intercept listed here (0.0016) correct? Also, it might be worth mentioning somewhere that you would expect the slope here to be roughly 2x that of the slope in Fig. 4 (which is what is actually seen), based on the way G and NCP are defined.*

Figure A3b has now been added to the main text as Figure 4b. The y-intercept is 1557.4, and this has been changed in the text. We also note in the Figure 4b caption, "As expected, the slope of TA versus DIC (0.31) is approximately twice that of G versus NCP (0.14). "

Discussion Comment from G. Diaz Pulida

We thank you for commenting on our discussion paper and for your suggestion to add the importance of live tissue in mediating calcification and dissolution. You bring up a very interesting point, and we have expanded on it and cited your paper in the discussion.

1 Secondary calcification and dissolution respond 2 differently to future ocean conditions.

3
4 **N. J. Silbiger¹ and M. J. Donahue¹**

5 [1] {University of Hawai‘i at Mānoa, Hawai‘i Institute of Marine Biology, PO Box 1346,
6 Kāne‘ohe, Hawai‘i, 96744}

7 Correspondence to: N.J. Silbiger (silbiger@hawaii.edu)

8 9 **Abstract**

10 Climate change threatens both the accretion and erosion processes that sustain coral reefs.
11 Secondary calcification, bioerosion, and reef dissolution are integral to the structural
12 complexity and long-term persistence of coral reefs, yet these processes have received
13 less research attention than reef accretion by corals. In this study, we use climate
14 scenarios from ~~RCP8.5~~RCP 8.5 to examine the combined effects of rising ocean acidity
15 and SST on both secondary calcification and dissolution rates of a natural coral rubble
16 community using a flow-through aquarium system. We found that secondary reef
17 calcification and dissolution responded differently to the combined effect of pCO₂ and
18 temperature. Calcification had a non-linear response to the combined effect of pCO₂-
19 temperature: the highest calcification rate occurred slightly above ambient conditions and
20 the lowest calcification rate was in the highest pCO₂-temperature condition. In contrast,
21 dissolution increased linearly with pCO₂-temperature. The rubble community switched
22 from net calcification to net dissolution at +~~272~~271 μatm pCO₂ and 0.~~84~~75° C above
23 ambient conditions, suggesting that rubble reefs may shift from net calcification to net

24 | dissolution before the end of the century. Our results indicate that (i) dissolution may be
25 | more sensitive to climate change than calcification, and (i) that calcification and
26 | dissolution have different functional responses to climate stressors, ~~highlighting; this~~
27 | highlights the need to study the effects of climate stressors on both calcification and
28 | dissolution to predict future changes in coral reefs.

29

30 | **1 Introduction**

31 | In 2013, atmospheric carbon dioxide ($\text{CO}_{2(\text{atm})}$) reached an unprecedented
32 | milestone of 400 ppm (Tans and Keeling, 2013), and this rising $\text{CO}_{2(\text{atm})}$ is increasing
33 | sea-surface temperature (SST) and ocean acidity (Caldeira and Wickett, 2003; Cubasch et
34 | al., 2013; Feely et al., 2004). Global SST has increased by 0.78°C since pre-industrial
35 | times (Cubasch et al., 2013), and it is predicted to increase by another $0.8\text{-}5.7^{\circ}\text{C}$ by the
36 | end of this century (Meinshausen et al., 2011; Van Vuuren et al., 2008; Rogelj et al.,
37 | 2012). The Hawai'i Ocean Time-series detected a 0.075 decrease in mean annual pH at
38 | Station ALOHA over the past 20 years (Doney et al., 2009) and there have been similar
39 | trends at stations around the world including the Bermuda Atlantic Time-series and the
40 | European Station for Time-series Observations in the ocean (~~DruppSolomon et al., 2013,~~
41 | 2007). pH is expected to drop by an additional 0.14-0.35 pH units by the end of the 21st
42 | century (Bopp et al., 2013). All marine ecosystems are at risk from rising SST and
43 | decreasing pH (Doney et al., 2009; Hoegh-Guldberg et al., 2007; Hoegh-Guldberg and
44 | Bruno, 2010), but coral reefs are particularly vulnerable to these stressors (reviewed in
45 | Hoegh-Guldberg et al., 2007).

46 Corals create the structurally complex calcium carbonate (CaCO₃) foundation of
47 coral reef ecosystems. This structural complexity is at risk from climate-driven shifts
48 from high-complexity, branched coral species to mounding and encrusting growth forms
49 (Fabricius et al., 2011) and from increases in the natural processes of reef destruction,
50 including bioerosion and dissolution (Wisshak et al., 2012, 2013; Tribollet et al., 2006).
51 While substantial research attention has focused on the response of reef-building corals to
52 climate change (reviewed in Hoegh-Guldberg et al., 2007; Fabricius, 2005; Pandolfi et al.,
53 2011), secondary calcification (calcification by non-coral invertebrates and calcareous
54 algae), bioerosion, and reef dissolution that are integral to maintaining the structural
55 complexity and net growth of coral reefs has received less attention (Andersson and
56 Gledhill, 2013; Andersson et al., 2011; Andersson and Mackenzie, 2012). Bioerosion and
57 dissolution breakdown the reef framework while secondary calcification helps maintain
58 reef stability by cementing the reef together (Adey, 1998; Camoin and Montaggioni,
59 1994; Littler, 1973) and producing chemical cues that induce settlement of many
60 invertebrate larvae including several species of corals (Harrington et al. 2004; Price
61 2010). Coral reefs will only persist if constructive reef processes (growth by corals and
62 secondary calcifiers) exceed destructive reef processes (bioerosion and dissolution). In
63 this study, we examine the combined effects of rising ocean acidity and SST on both
64 calcification and dissolution rates of a natural community of secondary calcifiers and
65 bioeroders.

66 Recent laboratory experiments have focused on the response of individual taxa of
67 bioeroders or secondary calcifiers to climate stressors. For example, studies have
68 specifically addressed the effects of rising ocean acidity and/or temperature on bioerosion

69 by a *Clionid* sponge (Wisshak et al., 2012, 2013; Fang et al., 2013) and a community of
70 photosynthesizing microborers (Tribollet et al., 2009; Reyes-Nivia et al., 2013). These
71 studies found that bioerosion increased under future climate change scenarios. Several
72 studies have focused on tropical calcifying algae and have found decreased calcification
73 (Semesi et al., 2009; Johnson et al., 2014; Comeau et al., 2013; Jokiel et al., 2008; Kleypas
74 and Langdon, 2006) and increased dissolution (Diaz-Pulido et al., 2012) with increasing
75 ocean acidity and/or SST. However, the bioeroding community is extremely diverse and
76 can interact with the surrounding community of secondary calcifiers: for example,
77 crustose coralline algae (CCA) can inhibit internal bioerosion (White, 1980; Tribollet and
78 Payri, 2001). To understand the combined response of bioeroders and secondary
79 calcifiers, we take a community perspective. ~~We and~~ examine the synergistic effects of
80 rising SST and ocean acidity, ~~modeled after the Representative Concentration Pathway~~
81 ~~(RCP) 8.5 climate scenario (Van Vuuren et al., 2011; Meinshausen et al., 2011)~~, on a
82 natural community of secondary calcifiers and bioeroders. Using the total alkalinity
83 anomaly technique, we test for net changes in calcification during the day and dissolution
84 (most of which is caused by bioeroders; ~~(Andersson and Gledhill, 2013);~~) at night. ~~RCP~~
85 ~~scenarios~~ Our climate change treatments are modelled after the Representative
86 Concentration Pathway (RCP) 8.5 climate scenario (Van Vuuren et al.,
87 2011; Meinshausen et al., 2011), one of the high emissions scenarios ~~that were~~ used in the
88 most recent Intergovernmental Panel on Climate Change (IPCC) report (Cubasch et al.,
89 2013). The ~~RCP~~ RCP 8.5 scenario predicts ~~that an increase in~~ temperature ~~will likely~~
90 increase by 3.8 – 5.7°C (Rogelj et al., 2012) and an increase in atmospheric CO₂ ~~will~~
91 increase by 557 ppm by the year 2100 (Meinshausen et al., 2011). We ~~chose to~~ use the

92 | ~~RCP8~~RCP 8.5 scenario because the current CO₂ concentrations are tracking just above
93 | what this scenario predicts (Sanford et al., 2014). While prior studies have focused on the
94 | contributions of individual community members, ~~to increased temperature and CO₂~~; here,
95 | we ~~test~~examine the community response to the ~~predicted RCP8~~RCP 8.5 climate scenario
96 | and measure ~~both calcification and~~ dissolution, ~~and net community production~~ rates.

97 | **2 Materials and Methods**

98 | **2.1 Collection Site**

99 | All collections were made on the windward side of Moku o Lo'e (Coconut Island)
100 | in Kāne'ohe Bay, Hawai'i adjacent to the Hawai'i Institute of Marine Biology. This
101 | fringing reef is dominated by *Porites compressa* and *Montipora capitata*, with occasional
102 | colonies of *Pocillopora damicornis*, *Fungia scutaria*, and *Porites lobata*. Kāne'ohe Bay
103 | is a protected, semi-enclosed embayment; the residence time can be >1 month long in the
104 | protected southern portion of the Bay (Lowe et al., 2009a;Lowe et al., 2009b) that is
105 | coupled with a high daily variance in pH (Guadayol et al., 2014). The wave action is
106 | minimal (Smith et al., 1981;Lowe et al., 2009a;Lowe et al., 2009b) and currents are
107 | relatively slow (5cm s⁻¹ maximum) and wind-driven (Lowe et al., 2009a;Lowe et al.,
108 | 2009b).

109 | **2.2 Sample Collection**

110 | We collected pieces of dead *Porites compressa* coral skeleton (hereafter, referred to as
111 | rubble) as representative communities of bioeroders and secondary calcifiers. Rubble was
112 | collected with a hammer and chisel from a shallow reef flat (~1m depth) in November,
113 | 2012. ~~Only pieces of rubble without any live coral were collected. The average (±SE)~~

114 | ~~skeletal density of the rubble was $1.53 \pm 0.012 \text{ g cm}^{-3}$ (n=85).~~ The rubble community in
115 | Kāneʻohe Bay is comprised of secondary calcifiers, including CCA from the genera
116 | *Hydrolithon*, *Sporolithon*, and *Peyssonnelia* and non-coral calcifying invertebrates (e.g.
117 | boring bivalves (*Lithophaga fasciola* and *Barbatia divaricate*), oysters (*Crassostrea*
118 | *gigas*), and small crustaceans); filamentous and turf algae; and internal bioeroders,
119 | including boring bivalves (*L. fasciola* and *B. divaricate*), sipunculids (*Aspidosiphon*
120 | *elegans*, *Lithacrosiphon cristatus*, *Phascolosoma perlucens*, and *Phascolosoma*
121 | *stephensoni*), phoronids (*Phoronis ovalis*), sponges (*Cliona* spp.) and a diverse
122 | assemblage of polychaetes (White, 1980). All rubble ~~was pieces were~~ combined after
123 | collection and maintained in a 100L flow-through tank with ambient seawater from
124 | Kāneʻohe Bay until random assignment to treatments.

Formatted: Font: Not Italic

125 | 2.3. Experimental Design

126 | The Hawaiʻi Institute of Marine Biology (HIMB) hosts a mesocosm facility with
127 | flow-through seawater from Kāneʻohe Bay and controls for light, temperature, pCO₂, and
128 | flow rate. The facility is comprised of 24 experimental aquaria split between four racks;
129 | each rack has ~~a 50L~~ 150L header tank which feeds 6 experimental aquaria, each 50L in
130 | volume (Figure 1).

131 | Before adding rubble to the experimental aquaria, we collected day and night
132 | samples of pH, total alkalinity (TA), temperature, and salinity from each aquarium during
133 | light and dark conditions all aquaria to demonstrate the stability of the system
134 | consistency of water conditions across aquaria without any rubble present (Table 1). The
135 | long-term temporal stability of the mesocosm system is reported in Putnam (2012). We

136 | then conducted “control” and “treatment” experiments to determine how ~~RCP8~~RCP 8.5
137 | predictions affect daytime calcification and nighttime dissolution rates in a natural rubble
138 | community. The first “control experiment” characterized baseline calcification and
139 | dissolution in each aquarium caused by differences in rubble communities. In the second
140 | “treatment experiment”, we manipulated pCO₂ and temperature to simulate four climate
141 | scenarios (pre-industrial, present day, 2050, and 2100) and tested the response of
142 | calcification ~~and dissolution.~~, dissolution, and net community production. Each
143 | experiment used the TA anomaly method (Smith and Key, 1975; Andersson et al., 2009).
144 | This method calculates net calcification from changes in total alkalinity, and calculates
145 | net community production from changes in total dissolved inorganic carbon adjusted for
146 | changes in carbon due to calcification. Because estimates of calcification are based on
147 | changes in total alkalinity, this method does not account for mechanical erosion (e.g.,
148 | small chips of CaCO₃ produced by sponge erosion). However, given the short duration of
149 | the experiment and the types of bioeroders present, we expect that chemical dissolution
150 | captured a significant proportion of the erosion in the system.

151 | Approximately 1.2L of rubble (~~3-4-5~~ pieces of ~~approximately equal size~~)weight
152 | 499 ± 148 g and skeletal density 1.53 ± 0.1 g cm⁻³ (mean ± SD, n=85)) were placed in
153 | each of the 24 experimental aquaria and acclimated to tank conditions in ambient
154 | seawater for three days. On the fourth day, we performed the control experiment,
155 | calculating daytime calcification and nighttime dissolution for rubble in ~~the~~ ambient
156 | seawater conditions using the TA anomaly technique ~~(Smith and Key, 1975).~~. The next
157 | day we manipulated seawater pCO₂ and temperature to replicate four climate scenarios
158 | for the treatment experiment ~~(Table 1)~~: pre-industrial (-1±0.057°C and -205±11.9 µatm),

159 present day (natural Kāneʻohe Bay seawater 24.8 ± 0.09 °C, 614 ± 15.6 μ atm), 2050
160 ($+1.4 \pm 0.09$ °C and $+255 \pm 31$ μ atm), and 2100 ($+2.4 \pm 0.08$ and $+433 \pm 40$ μ atm). Note that
161 all changes in temperature and pCO₂ were made relative to present day Kāneʻohe Bay
162 seawater conditions: pCO₂ in Kāneʻohe Bay is consistently high relative to the open
163 ocean and can range from 196-976 μ atm in southern Kāneʻohe bay depending on
164 conditions (Drupp et al., 2013). The yearly average pCO₂ at our collection site ranged
165 from 565-675 μ atm (Silbiger et al., ~~in review~~2014). After an acclimation time of seven
166 days, we sampled the treatment experiment, calculating daytime calcification and
167 nighttime dissolution over a 24 hour period.

168 During both experiments, TA, pH, salinity, temperature, and dissolved inorganic
169 nutrient (DIN) samples were collected every 12 hours over a 24 hour period ~~(total of~~
170 ~~three times)~~; just before lights-on in the morning (time 1) and just before lights-off at
171 night (time 2) to capture light conditions, and then again before lights-on the next
172 morning (time 3) to capture dark conditions. Flow into each aquarium was monitored and
173 adjusted every three hours to ensure a consistent flow rate over the 24 hour experiment.
174 We calculated net ecosystem calcification ~~and~~ dissolution, and net community
175 production using a simple box model (Andersson et al., 2009) and normalized all our
176 calculations to the surface area of the rubble in each tank. Surface area of the rubble was
177 calculated using the wax dipping technique (Stimson and Kinzie III, 1991) at the end of
178 the experiment.

2.4 Laboratory Mesocosm Set-up

The mesocosm facility (Figure 1) is supplied with ambient seawater from Kāneʻohe Bay, which is filtered through a sand filter, passed through a water chiller (Aqualogic Multi Temp MT-1 Model # 2TTB3024A1000AA), and then fed into one of the four header tanks. pCO₂ was manipulated using a CO₂ gas blending system (see Fanguie et al., 2010; Johnson and Carpenter, 2012). Each target pCO₂ concentration was created by mixing CO₂-free atmospheric air with pure CO₂ using mass flow controllers (C100L Sierra Instruments). Output pCO₂ was analyzed using a calibrated infrared CO₂ analyzer (A151, Qubit Systems). CO₂ mixtures were then bubbled into one of the four header tanks and water from each individual header tank fed into the six individual treatment aquaria (Figure 1). The pCO₂ in each treatment aquarium was estimated with CO₂SYN (Van Heuven et al., 2009) using pH and TA as the parameters.

Temperature was manipulated in each treatment aquarium using dual-stage temperature controllers (Aqualogic TR115DN). The temperature was continuously monitored with temperature loggers (TidbiT v2 Water Temperature Data Logger, sampling every 20 min) and point measurements were taken during every sampling period with a handheld digital thermometer (Traceable Digital Thermometer, Thermo Fisher Scientific; precision = 0.001 °C). Light was controlled by positioning an oscillating pendant metal-halide light (250 W) over a set of three aquaria and was programmed to emit an equal amount of light to each tank (~500μE of light). Lights were set to a 12:12 hour photoperiod and were monitored using a LI-COR spherical quantum PAR sensor. Flow rate was maintained at 115±1 ml min⁻¹, resulting in a residence time of

201 7.3±0.07 hours per tank. Each aquarium was equipped with a submersible powerhead
202 pump (Sedra KSP-7000 powerhead) to ensure that the tank was well-mixed.

203 **2.5 Seawater Chemistry**

204 All sample collection and storage vials were cleaned in a 10% HCl bath for 24 hours and
205 rinsed three times with MilliQ water before use and rinsed three times with sample water
206 during sample collection and processing.

207 **2.5.1 Total Alkalinity**

208 Duplicate TA samples were collected in 300 ml borosilicate sample containers with glass
209 stoppers. Each sample was preserved with 100µL of 50% saturated HgCl₂ and analyzed
210 within 3 days using open cell potentiometric titrations on a Mettler T50 autotitrator
211 (Dickson et al., 2007). A Certified Reference Material (CRM - Reference Material for
212 Oceanic CO₂ Measurements, A. Dickson, Scripps Institution of Oceanography) was run
213 at the beginning of each sample set ~~to ensure the~~ The accuracy of the titrator. ~~Our~~
214 accuracy was better never deviated more than ±0.8%, ~~% from the standard,~~ and ~~our~~ TA
215 measurements were corrected for these deviations. The precision was 3.55µEq (measured
216 as standard deviation of the duplicate water samples). During the 24-hour control
217 experiment the average changes in TA were 37µEq over the day and 20µEq over the
218 night (day and night TA changes were of larger magnitude in the treatment experiments):
219 these are measurable changes given the precision and accuracy of the TA measurements.

Formatted: Font color: Auto

220 **2.5.2 pH_t (total scale)**

221 Duplicate pH_t samples were collected in 20ml borosilicate glass vials, brought to a
222 constant temperature of 25°C in a water bath, and immediately analyzed using an m-

223 | cresol dye addition spectrophotometric technique- (Dickson et al., 2007). Accuracy of the
224 | pH was tested against a Tris buffer of known pH_i from the Dickson Lab at Scripps
225 | Institution of Oceanography (Dickson et al., 2007). Our accuracy was better than
226 | $\pm 0.04\%$, and the precision was 0.004 pH units (measured as standard deviation of the
227 | duplicate water samples). *In situ* pH and the remaining carbonate parameters were
228 | calculated using CO2SYS (Van Heuven et al., 2009) with the following measured
229 | parameters: pH_i, TA, temperature, and salinity. The K₁K₂ apparent equilibrium constants
230 | were from Mehrbach (1973) and refit by Dickson & Millero (1987) and HSO₄⁻
231 | dissociation constants were taken from Uppström (1974) and Dickson (1990).

232 | **2.5.3 Salinity**

233 | Duplicate salinity samples were analyzed on a Portasal 8410 portable salinometer ~~which~~
234 | ~~was~~ calibrated with an OSIL IAPSO standard (accuracy = ± 0.003 psu, precision =
235 | ± 0.0003 psu).

236 | **2.5.4 Nutrients**

237 | Nutrient samples were collected with 60ml plastic syringes and immediately filtered
238 | through combusted 25mm glass fiber filters (GF/F 0.7 μ m) and transferred into 50ml
239 | plastic centrifuge tubes. Nutrient samples were frozen and later analyzed for Si(OH)₄,
240 | NO₃⁻, NO₂⁻, NH₄⁺, and PO₄³⁻ on a Seal Analytical AA3 HR Nutrient Analyzer at the UH
241 | SOEST Lab for Analytical Chemistry.

242 | **2.6 Measuring Net Ecosystem Calcification**

243 | We assumed that the mesocosms were well mixed systems; thus, we calculated net
244 | ecosystem calcification and net community photosynthesis following the simple box
245 | model presented in Andersson et al. (2009). TA was ~~first~~ normalized to a constant

Formatted: Indent: First line: 0"

246 salinity (35 psu) ~~and to [DIN]~~ to account for changes ~~in TA~~ due to evaporation and
247 ~~photosynthesis/respiration, respectively, then corrected for dissolved inorganic nitrogen~~
248 ~~and phosphate to account for their small contributions to the acid-base system (Wolf-~~
249 ~~Gladrow et al., 2007).~~ Net ecosystem calcification, or G, was calculated using the
250 following equation:

251

$$G = \left[F_{TAin} - F_{TAout} - \frac{dTA}{dt} \right] / 2 \quad \text{Eq. 1}$$

Formatted: Left

252 ~~where F_{TAin} is the rate of TA flowing into an aquarium (= average TA in the aquaria,~~
253 ~~F_{TAout} header tank times the inflow rate). F_{TAout} is the rate of TA flowing out of the~~
254 ~~aquaria, an aquarium (= average TA in the aquarium times the outflow rate), and ,~~
255 ~~$\frac{dTA}{dt}$ is the change in TA in the aquaria per unit time in $\text{mmol CaCO}_3 \text{ m}^{-2} \text{ hr}^{-1}$ an~~
256 ~~aquarium during the measurement period (change in TA normalized to the volume of~~
257 ~~water and the surface area of the rubble); specific calculations are given in the~~
258 ~~supplemental material.~~ The equation is divided by two because one mole of CaCO_3 is
259 precipitated or dissolved for every two moles of TA removed or added to the water
260 column. Here, G represents the sum of all the calcification processes minus the sum of all
261 the dissolution processes in $\text{mmol CaCO}_3 \text{ m}^{-2} \text{ hr}^{-1}$; thus, all positive numbers are net
262 calcification, and all negative numbers are negative net calcification (i.e., net dissolution).
263 Net daytime calcification (G_{day}) is calculated from the first 12 hour sampling period in
264 the light, net nighttime dissolution (G_{night}) is calculated from the second 12 hour sampling
265 period in the dark, and total net calcification (G_{net}) is calculated from the full 24 hour

266 cycle ($G_{\text{day}} + G_{\text{night}}$). All rates are G_{day} , G_{night} , and G_{net} are converted from hourly to daily
267 rates and presented as $\text{mmol CaCO}_3 \text{ m}^{-2} \text{ d}^{-1}$.

268 **2.7 Measuring Net Community Production and Respiration**

269 Net community production (NCP) was calculated by measuring changes in DIC (Gattuso
270 et al., 1999). DIC was normalized to a constant salinity (35 psu) to account for any
271 evaporation over the 24 hour period. We used a simple box model to calculate NCP:

$$NCP = \left[F_{\text{DICin}} - F_{\text{DICout}} - \frac{d\text{DIC}}{dt} \right] - G$$

Eq. 2

272 F_{DICin} , F_{DICout} , and $\frac{d\text{DIC}}{dt}$ are the rates of DIC flowing into the aquaria, flowing out of the
273 aquaria, and the change in DIC in the aquaria per unit time in $\text{mmol C m}^{-2} \text{ hr}^{-1}$,
274 respectively. To measure NCP, we subtract G to remove any change in carbon due to
275 inorganic processes. NCP represents the sum of all the photynthetic processes minus the
276 sum of all the respiration processes, thus all positive numbers are net photosynthesis and
277 all negative numbers are negative net photosynthesis (i.e., net respiration). Net daytime
278 NCP (NCP_{day}) is calculated from the first 12 hour sampling period in the light, net
279 nighttime NCP (NCP_{night}) is calculated from the second 12 hour sampling period in the
280 dark, and total NCP (NCP_{net}) is calculated from the full 24 hour cycle ($NCP_{\text{day}} \pm$
281 NCP_{night}). All rates are presented as $\text{mmol C m}^{-2} \text{ d}^{-1}$.

282 **2.8 Statistical Analysis**

283 Each aquarium contained a slightly different rubble community because of the
284 randomization of rubble pieces to each treatment. To ensure there were no systematic
285 differences in rubble communities between racks (rack effects) before the experimental

286 | treatments were applied, we tested for differences in G_{day} , G_{night} , calcification and
287 | G_{net} , NCP between racks in the control experiment using an ANOVA. (Figure A2).

288 | In the treatment experiment, we first tested for feedbacks in carbonate chemistry
289 | due to the presence of rubble: using a paired t-test, we compared the day-night difference
290 | in measured $p\text{CO}_2$ in each aquarium with rubble, $(p\text{CO}_{2,\text{day}} - p\text{CO}_{2,\text{night}})_{\text{rubble}}$, and
291 | without rubble, $(p\text{CO}_{2,\text{day}} - p\text{CO}_{2,\text{night}})_{\text{no rubble}}$. ~~Because of~~

292 | Although we imposed four discrete temperature- $p\text{CO}_2$ scenario treatments on
293 | each tank (Table 1), random variation between treatments and the feedback between the
294 | rubble communities and the water chemistry resulted in near-continuous variation in
295 | $p\text{CO}_2$ and temperature- $p\text{CO}_2$ treatments across treatments and the significant feedbacks in
296 | the water chemistry due to the presence of rubble aquaria (Figures 2 and A1), a
297 | regression using the actual). To capture this continuous variation in temperature- $p\text{CO}_2$ in
298 | the analysis, we used the measured temperature- $p\text{CO}_2$ seawater condition was more
299 | informative than an ANOVA using the imposed seawater condition in testing as a
300 | continuous independent variable in a regression rather than the four categorical treatment
301 | conditions in an ANOVA (an analysis of G and NCP using the ANOVA approach is
302 | included in Figures A3, A4 and Tables A1, A2). The regression approach allowed us to
303 | better capture the quantitative relationships between net calcification (G) and treatment.
304 | Therefore, we used a regression to test for linear and non-linear relationships between
305 | day, night, or NCP and net calcification (G_{day} , G_{night} , and G_{net}) and our independent
306 | variable: change in $p\text{CO}_2 \times$ temperature from background seawater conditions (hereafter,
307 | referred to as the temperature- $p\text{CO}_2$ treatment. We created a single, continuous variable,

308 ~~Standardized Climate Change). (Results using an ANOVA design are included as~~
 309 ~~supplemental materials: Figure A2, Table A1). Standardized Climate Change was~~
 310 ~~calculated as (SCC), from a linear combination of temperature and pCO₂ values in~~
 311 ~~each Treatment Experiment pCO_{2,i} × Temperature_i) (Control Experiment pCO_{2,i} ×~~
 312 ~~Temperature_i), where *i* represents an individual aquarium. A simple productlinear~~
 313 ~~combination~~ was used because pCO₂ increased linearly with temperature (Figure 2). We
 314 ~~), as imposed by our treatments. We first calculated the relationship between ΔTemp (Eq~~
 315 ~~3) and ΔpCO₂ (Eq 4) using linear regression. The coefficients from this regression (slope:~~
 316 ~~α = 0.0031; y-intercept: β = - 0.078) were used to combine pCO₂ and temperature onto~~
 317 ~~the same scale, as a measure of Standardized Climate Change (Eq 5):~~

$$\Delta Temp_i = Temp_{trt,i} - Temp_{cont,i} \quad \text{Eq. 3}$$

$$\Delta pCO_{2i} = pCO_{2trt,i} - pCO_{2cont,i} \quad \text{Eq. 4}$$

$$SCC_i = \Delta Temp_i + \alpha * \Delta pCO_{2i} + \beta \quad \text{Eq. 5}$$

321 ~~This synthetic temperature-pCO₂ axis, SCC, is centered the data around on~~ the ambient
 322 ~~(control) conditions such that a value of 0 in the independent variable (Standardized~~
 323 ~~Climate Change) corresponds to present day Kāne‘ohe Bay conditions, a negative value~~
 324 corresponds to water that is colder and less acidic (pre-industrial) and a positive value
 325 corresponds to water that is warmer and more acidic (future conditions) compared to
 326 background seawater. ~~(The independent relationships between G and NCP with ΔTemp~~
 327 ~~and ΔpCO₂ are shown in Figures A5 and A6 and are similar to the relationship with~~
 328 ~~SCC.)~~

Formatted: Font color: Auto

Formatted: Font color: Auto

Formatted: Font color: Auto

Formatted: Indent: First line: 0"

329 With SCC as a continuous, independent variable, we used a regression to test for
330 linear and non-linear relationships between day, night, and net calcification (G_{day} , G_{night} ,
331 and G_{net}) and NCP (NCP_{day} , NCP_{night} , and NCP_{net}) versus SCC. For a simple test of
332 nonlinearity in the response of calcification to ~~standardized climate change~~ SCC, we
333 included a quadratic term (~~(Standardized Climate Change)²~~ (SCC²) in the model. For G_{day} ,
334 we used weighted regression (~~Fair, 1974~~) weight function: $w_i = 1/(1+|r_i|)$, where w_i =
335 weight and r_i = residual~~), Fair, 1974~~) to account for heteroscedasticity. All other data met
336 assumptions for a linear regression. Lastly, we used a linear regression to test the
337 relationship between G and NCP.

338
339

340 **3 Results**

341 **3.1 Control Experiment**

342 For rubble in ambient seawater conditions, the average G_{day} , G_{night} , and G_{net} in the control
343 experiment were $3.4 \pm 0.16 \text{ mmol m}^{-2} \text{ d}^{-1}$, $-2.4 \pm 0.15 \text{ mmol m}^{-2} \text{ d}^{-1}$, and $0.96 \pm 0.20 \text{ mmol m}^{-2} \text{ d}^{-1}$, respectively. There was no significant difference in G_{day} ($F_{3,23}=0.68$, $p=0.58$), G_{night}
344 ($F_{3,23}=1.52$, $p=0.24$), or G_{net} ($F_{3,23}=1.38$, $p=0.28$) between racks in the control experiment
345 (Figure A2). NCP rates also did not show any racks effects. Average NCP rates were
346 $23.2 \pm 1.4 \text{ mmol m}^{-2} \text{ d}^{-1}$ ($F_{3,23}=0.07$, $p=0.94$) during the day, $-20.7 \pm 1.9 \text{ mmol m}^{-2} \text{ d}^{-1}$
347 ($F_{3,23}=1.95$, $p=0.15$) during the night, and $2.5 \pm 2.1 \text{ mmol m}^{-2} \text{ d}^{-1}$ ($F_{3,23}=1.5$, $p=0.25$) over
348 the entire 24 hour period.

349

350 3.2 Treatment Experiment

351 The rubble communities significantly altered the seawater chemistry, with higher pCO₂
352 than the applied pCO₂ manipulation, particularly at night (Figure A1). The mean
353 difference between day and night pCO₂ for all treatments was 134.4 ± 39 µatm without
354 rubble and was 438.5 ± 163.9 µatm when rubble was present (t₂₃ = -7.23, p < 0.0001;
355 Figure 2).

356 Standardized Climate Change was a significant predictor for G_{day}, G_{night}, and G_{net}
357 (Table 2; Figure 3). G_{day} had a non-linear relationship with Standardized Climate Change
358 (Table 2, Figure 3a), increasing to a threshold and then rapidly declining. G_{night}, however,
359 had a strong linear relationship with Standardized Climate Change (Table 2; Figure
360 ~~3b3c~~), suggesting that joint increases in ocean pCO₂ and temperature will increase ~~night~~
361 ~~time~~ nighttime dissolution of coral rubble. Lastly, G_{net} had a strong negative relationship
362 with Standardized Climate Change (Table 2; Figure ~~3e3e~~) and the rubble community
363 switched from net calcification to net dissolution at an increase in pCO₂ and temperature
364 of 271.6 µatm and 0.8475° C, respectively. Standardized Climate Change was also a
365 significant predictor of NCP: Day, night, and net NCP rates all declined with
366 standardized climate change (Table 2; Figure 3b,d,f; Figure3).

367 ~~G and NCP were significantly correlated (Net ecosystem calcification increased~~
368 ~~with net community production (F_{1,46} = 260, p < 0.0001, R² = 0.85; Figure 4 and Figure~~
369 ~~A3).~~ In general, ~~rubble that was~~ communities were net photosynthesizing ~~was also~~ and net
370 calcifying ~~and rubble that was~~ during the day (Figure 4a: squares in the upper right
371 ~~quadrant) and were~~ net respiring ~~was also~~ and net dissolving ~~at night (Figure 4a: circles~~

372 in the lower left quadrant). The exception was ~~rubble experiencing communities in~~ the
373 most extreme temperature-pCO₂ treatment, ~~which was: these communities were~~ net
374 respiring during the day while ~~still~~ holding a positive, yet very low, calcification rate.
375 (Figure 4a: squares in the upper left quadrant).
376

377 4 Discussion

378 4.1 Carbonate Chemistry Feedbacks

379 The rubble communities in the aquaria significantly altered the seawater
380 chemistry, particularly at night ($t_{23} = -7.23$, $p < 0.0001$; Figure 2, Figure A1). This day-
381 night difference in seawater chemistry increased under more extreme climate scenarios,
382 as predicted by Jury *et al.* (2013). This large diel swing in pCO₂ is not uncommon on
383 shallow coral reef environments. pCO₂ ranged from 480 to 975 μatm over 24 hours on a
384 shallow reef flat adjacent to our collection site (Silbiger *et al.* ~~*in review*~~, 2014) and pCO₂
385 ~~ranged~~ from 450 to 742 μatm on a Moloka'i reef flat dominated by coral rubble (Yates
386 and Halley, 2006). Here, pCO₂ had an average difference of 438 μatm between day and
387 night with a range of 412 μatm in the pre-industrial treatment to 854 μatm in the most
388 extreme ~~pCO₂~~ × temperature-pCO₂ treatments (Figure 2). In our study, we incorporated
389 these feedbacks into the statistical analysis by using the actual, sampled pCO₂ (and
390 temperature) in each aquaria (Figure 3) rather than using the intended pCO₂ (and
391 temperature) treatments in an ANOVA (~~Table~~ Tables A1, Figure A2 and Figures A3, A4),
392 better reflecting the pCO₂ experienced by organisms in each aquarium.

4.2 Calcification ~~and~~, Dissolution, and Net Community Production in a High CO₂ and Temperature Environment

Our results suggest that as pCO₂ and temperature increase over time, rubble reefs may shift from net calcification to net dissolution. In our study, this tipping point occurred at a pCO₂ and temperature increase of 271.6 μatm and 0.8475° C. Further, our results showed that G_{day} and G_{night} in a natural coral rubble community have different functional responses to changing pCO₂ and temperature (Figure 3). The ranges in G_{day} and G_{night} in our aquaria were similar to *in situ* rates on Hawaiian rubble reefs. Yates & Halley (2006) saw G_{day} values between ~~0.263.3~~ to ~~0.9811.7~~ mmol CaCO₃ m⁻² h~~r~~d⁻¹ and G_{night} values between ~~-0.2.4~~ to ~~-3.024~~ mmol CaCO₃ m⁻² h~~r~~d⁻¹ on a Moloka'i reef flat with only coral rubble. (Note that Yates and Halley calculated G over a 4 hour timeframes and the data was multiplied by 3 here to show G in mmol m⁻² d⁻¹. Also note that we normalized our rates to the surface area of the rubble while Yates and Halley (2006) normalized their rates to planar surface area.) G_{day} and G_{night} in our experiment ranged from ~~0.161.9~~ to ~~0.789.4~~ and ~~-0.1.3~~ to ~~-10~~ to ~~-0.87.5~~ mmol CaCO₃ m⁻² h~~r~~d⁻¹, respectively, across all treatment conditions. The higher dissolution rates in the *in situ* study by Yates and Halley (2006) are likely due to dissolution in the sediment, which was not present in our study.

G_{day} had a non-linear response to Standardized Climate Change. G_{day} increased with ~~pCO₂ × temperature-pCO₂~~ until slightly above ambient conditions, and then decreased under more extreme climate conditions (Figure 3a). This mixed response, increasing and then decreasing with Standardized Climate Change, is reflected in prior experiments. We suggest ~~two~~three possible mechanisms to explain why calcification

Formatted: Subscript

416 | increases in slightly higher ~~pCO₂~~ × temperature-~~pCO₂~~ than ambient conditions. 1) Some
417 | calcifiers can maintain and even increase their calcification rates in acidic conditions
418 | (Kamenos et al., 2013; Findlay et al., 2011; Rodolfo-Metalpa et al., 2011; Martin et al.,
419 | 2013) by either modifying their local pH environment (Hurd et al., 2011) or partitioning
420 | their energetic resources towards calcification (Kamenos et al., 2013). For example, in
421 | low, stable pH conditions the coralline algae, *Lithothamnion glaciale*, increased its
422 | calcification rate relative to a control treatment but, did not concurrently increase its rate
423 | of photosynthesis (Kamenos et al., 2013). Kamenos et al (2013) suggest that the up-
424 | regulation of calcification may limit photosynthetic efficiency. In the present study, the
425 | increase in G_{day} coincided with a decrease in net photosynthesis- (Figure 3a,b).
426 | Photosynthesizing calcifiers in the community may be partitioning their energetic
427 | resources more towards calcification and away from photosynthesis in order to maintain a
428 | positive calcification rate (Kamenos et al., 2013). Notably, turf algae likely have a major
429 | control over the NCP in this community which would not have any impact on
430 | calcification. 2) An alternative hypothesis is that the calcifiers may be adapted or
431 | acclimatized to high pCO₂ conditions (Johnson et al., 2014) and have not yet reached
432 | their threshold because the rubble was collected from a naturally high and variable pCO₂
433 | environment (Guadayol et al., 2014); Silbiger et al. 2014). 3) In this study, the calcifiers
434 | experienced a combined increase in both pCO₂ and temperature and, thus, the non-linear
435 | response in G_{day} may also be due a metabolic response. In a typical thermal performance
436 | curve, organisms increase their metabolism until they have reached a thermal maximum
437 | and then rapidly decline (Huey and Kingsolver, 1989; Pörtner et al., 2006), and we see
438 | this response in our results. A recent study found a similar nonlinear response to

439 temperature and pCO₂ in the coral *Siderastrea sidera* (Castillo et al. 2014). While they
440 attribute the pCO₂ response to photosynthesis being neutralized (we did not see this
441 response in our non-coral community), they suggest that the thermal response is due to
442 both changes in metabolism and thermally-driven changes in aragonite saturation state
443 (Castillo et al. 2014).

444 We saw a decline in both calcification and photosynthesisNCP in the extreme
445 pCO₂ × temperature-pCO₂ condition- (Figure 3). Calcification has been shown to decline
446 with climate stressors and the magnitude of decline differs across species (Kroeker et al.,
447 2010; Pandolfi et al., 2011; Ries et al., 2009; Kroeker et al., 2013). The concurrent decline
448 in photosynthesisNCP and calcification (Figure 3a,b & 4) suggests that non-
449 photosynthesizing invertebrates in the community (such as bivalves) might be dominating
450 the calcification signal in these conditions. This hypothesis would explain the pattern that
451 we see in Figure 4, where communities in the most extreme pCO₂ and temperature
452 conditions are net respiring during the day while still maintaining a small, positive
453 calcification rate- (Figure 4a: five points in the upper left quadrant).

454 G_{night} rates are more straightforward, decreasing linearly with pCO₂ and
455 temperature (Figures ~~3b~~3c and 4). NCP_{night} rates also decreased linearly with pCO₂ and
456 temperature (Figure 3d). Similarly, Andersson et al. (2009) saw an increase in dissolution
457 under acidic conditions in a community of corals, sand, and CCA. Previous studies on
458 individual bioeroder taxa have also found higher rates of bioerosion or dissolution in
459 more acidic, higher temperature conditions (Wisshak et al., 2013; Fang et al., 2013; Reyes-
460 Nivia et al., 2013; Tribollet et al., 2009; Wisshak et al., 2012). Studies, including the
461 present one, that focused on community-level responses There are several mechanisms

Formatted: Font color: Auto, Border: : (No border)

Formatted: Subscript

462 that could be mediating the increased dissolution rates in the high temperature-pCO₂
463 treatments: 1) Higher temperatures could increase the metabolism of the bioeroder
464 community, thus increasing borer activity (e.g., Davidson et al. 2013). 2) Because many
465 boring organisms excrete acidic compounds to erode the skeletal structure (Hutchings
466 1986), reduced pH in the overlaying water column may reduce the metabolic cost to the
467 organisms, making it easier for eroders to breakdown the CaCO₃. 3) Higher dissolution
468 rates could be mediated by an increase in the proportion of dolomite in the skeletal
469 structure of CCA on the rubble. A recent study found a 200% increase in dolomite in
470 CCA that was exposed to high pCO₂ and temperature conditions; this increase in
471 dolomite resulted in increased bioerosion by endolithic algae (Diaz-Pulido et al., 2014).
472 However, it is unlikely that changes in the mineralogy of the CCA indirectly increased
473 dissolution here given the short time-scale of our study. In the present study, we used the
474 TA anomaly method to calculate chemical dissolution as a proxy for bioerosion. Future
475 studies should also include measures of mechanical breakdown (e.g. the production of
476 sponge chips) in addition to chemical dissolution for a more complete picture of the
477 impacts of climate stress on reef breakdown. Studies, including the present one, which
478 focused on community-level responses, have consistently found that ocean acidification
479 will increase dissolution rates on coral reefs (Andersson and Gledhill, 2013).

480 ~~Dissolution was more strongly affected by~~ Standardized Climate Change
481 explained more of the variance in dissolution than in calcification: in our rubble
482 community: ($R_{night}^2 = 0.64 > R_{day}^2 = 0.33$; Table 2) this result is not surprising.
483 Bioerosion, an important driver of dissolution, may be more sensitive to changes in ocean

Formatted: Border: : (No border)

484 acidity than calcification, leading to net dissolution in high CO₂ waters. Many boring
485 organisms excrete acidic compounds, which may be less metabolically costly in a low pH
486 environment. Erez et al. (2011) hypothesize that increased dissolution, rather than
487 decreased calcification, maybe be the reason that net coral reef calcification is sensitive to
488 ocean acidification. The results of this study support this hypothesis. Although G_{net}
489 declines linearly with pCO₂-temperature, calcification (G_{day}) and dissolution (G_{night}) have
490 distinct responses to Standardized Climate Change: G_{day} had a non-linear response while
491 G_{night} declined linearly with Standardized Climate Change. Our results highlight the need
492 to study the effects of climate stressors on both calcification and dissolution.

Formatted: Border: : (No border)

493 **Author contributions:**

494 Conceived and designed the experiments: NJS MJD. Performed the experiments: NJS.
495 Analyzed the data: NJS MJD. Wrote the paper: NJS MJD.

496 **Acknowledgements**

497 Thanks to I Caldwell, R Coleman, J Faith, K Hurley, J Miyano, R Maguire, D. Schar,
498 ~~JJM~~ Sziklay, and MM Walton for help in field collections and lab analyses and to R.
499 Briggs from UH SOEST Lab for Analytical Chemistry. MJ Atkinson, R. Gates, C Jury, H
500 Putnam, and R Toonen gave thoughtful advice throughout the project. Comments by F.
501 Mackenzie and our two anonymous reviewers improved this manuscript. This project
502 was supported by a NOAA Dr. Nancy Foster Scholarship to N.J.S., a PADI Foundation
503 Grant to N.J.S., and Hawaii SeaGrant 1847 to MJD. ~~This is HIMB contribution #xxxx,~~
504 ~~Hawai'i SeaGrant contribution #xxx, and SOEST #xxxx~~ This paper is funded in part by a
505 grant /cooperative agreement from the National Oceanic and Atmospheric
506 Administration, Project R/IR-18, which is sponsored by the University of Hawaii Sea

507 | Grant College Program, SOEST, under Institutional Grant No. NA09OAR4170060 from
508 | NOAA Office of Sea Grant, Department of Commerce. The views expressed herein are
509 | those of the author(s) and do not necessarily reflect the views of NOAA or any of its
510 | subagencies. This is HIMB contribution #1607, Hawai'i SeaGrant contribution # UNIHI-
511 | SEAGRANT-JC-12-19, and SOEST #9237.
512 |

513 **References**

- 514 | [Adey, W.H. Review—coral reefs: algal structures and mediated ecosystems in shallow](#)
515 | [turbulent, alkaline waters. *Journal of Phycology*, 34, 393-406, 1998.](#)
- 516 Andersson, A. J., Kuffner, I. B., Mackenzie, F. T., Jokiel, P. L., Rodgers, K. S., and Tan,
517 A.: Net Loss of CaCO₃ from a subtropical calcifying community due to seawater
518 acidification: mesocosm-scale experimental evidence, *Biogeosciences*, 6, 1811-1823,
519 2009.
- 520 Andersson, A. J., Mackenzie, F. T., and Gattuso, J.-P.: Effects of ocean acidification on
521 benthic processes, organisms, and ecosystems, in: *Ocean Acidification*, edited by:
522 Gattuso, J.-P., and Hansson, L., Oxford University Press, 122-153, 2011.
- 523 Andersson, A. J., and Mackenzie, F. T.: Revisiting four scientific debates in ocean
524 acidification research, *Biogeosciences*, 9, 893-905, 2012.
- 525 Andersson, A. J., and Gledhill, D.: Ocean Acidification and Coral Reefs: Effects on
526 Breakdown, Dissolution, and Net Ecosystem Calcification, *Annual Review of Marine*
527 *Science*, Vol 5, 5, 321-348, 2013.
- 528 Bopp, L., Resplandy, L., Orr, J. C., Doney, S. C., Dunne, J. P., Gehlen, M., Halloran, P.,
529 Heinze, C., Ilyina, T., Séférian, R., Tjiputra, J., and Vichi, M.: Multiple stressors of ocean
530 ecosystems in the 21st century: projections with CMIP5 models, *Biogeosciences*, 10,
531 3627-3676, 2013.
- 532 Caldeira, K., and Wickett, M. E.: Oceanography: anthropogenic carbon and ocean pH,
533 *Nature*, 425, 365-365, 2003.
- 534 | [Camoin, G.F., Montaggioni, L.F., High energy coralg-al-stromatolite frameworks from](#)
535 | [Holocene reefs \(Tahiti, French Polynesia\), *Sedimentology*, 41, 656-676, 1994.](#)
- 536 | [Castillo, K.D., Ries, J.B., Bruno, J.F., Westfield, I.T., The reef-building coral *Siderastrea*](#)
537 | [*siderea* exhibits parabolic responses to ocean acidification and warming. *Proc. R. Soc. B.*,](#)
538 | [281, 20141856, 2014](#)
- 539 Comeau, S., Edmunds, P. J., Spindel, N. B., and Carpenter, R. C.: The responses of eight
540 coral reef calcifiers to increasing partial pressure of CO₂ do not exhibit a tipping point,
541 *Limnol. Oceanogr.*, 58, 388-398, 2013.
- 542 Cubasch, U., Wuebbles, D., Chen, D., Facchini, M. C., Frame, D., Mahowald, N., and
543 Winther, J.-G.: *Climate Change 2013: The Physical Science Basis. Contribution of*
544 *Working Group I to the Fifth Assessment Report of the Intergovernmental Panel on*
545 *Climate Change Cambridge, United Kingdom and New York, NY, USA. , 2013.*
- 546 | [Davidson, T.M., de Rivera, C.E., Carlton, J.T., Small increases in temperature exacerbate](#)
547 | [the erosive effects of a non-native burrowing crustacean, *Journal of Experimental Marine*](#)
548 | [*Biology and Ecology*, 446, 115-121, 2013.](#)
- 549 Diaz-Pulido, G., Anthony, K., Kline, D. I., Dove, S., and Hoegh-Guldberg, O.:
550 Interactions between ocean acidification and warming on the mortality and dissolution of
551 coralline alge, *Journal of Phycology*, 48, 32-39, 2012.

552 [Diaz-Pulido, G., Nash, M.C., Anthony, K.R.N., Bender, D., Opdyke, B.N., Reyes-Nivia,](#)
553 [C., Troitzsch, U., Greenhouse conditions induce mineralogical changes and dolomite](#)
554 [accumulation in coralline algae on tropical reefs, *Nature Communications*, 5, 3310,](#)
555 [DOI:10.1038/ncomms4310, 2014](#)

556 Dickson, A. G., and Millero, F. J.: A comparison of the equilibrium constants for the
557 dissociation of carbonic acid in seawater media, *Deep Sea Research Part A*.
558 *Oceanographic Research Papers*, 34, 1733-1743, 1987.

559 Dickson, A. G.: Standard potential of the reaction: $\text{AgCl (s)} + 12\text{H}_2(\text{g}) = \text{Ag (s)} + \text{HCl (aq)}$,
560 and the standard acidity constant of the ion HSO_4^- in synthetic sea water from 273.15
561 to 318.15 K, *The Journal of Chemical Thermodynamics*, 22, 113-127, 1990.

562 Dickson, A. G., Sabine, C. L., and Christian, J. R.: Guide to best practices for ocean CO₂
563 measurements, 2007.

564 Doney, S. C., Fabry, V. J., Feely, R. A., and Kleypas, J. A.: Ocean Acidification: The
565 Other CO₂ Problem, *Annual Review of Marine Science*, 1, 169-192, 2009.

566 Drupp, P. S., De Carlo, E. H., Mackenzie, F. T., Sabine, C. L., Feely, R. A., and
567 Shamberger, K. E.: Comparison of CO₂ dynamics and air-sea gas exchange in differing
568 tropical reef environments, *Aquatic Geochemistry*, 19, 371-397, 2013.

569 Erez, J., Reynaud, S., Silverman, J., Schneider, K., and Allemand, D.: Coral calcification
570 under ocean acidification and global change, in: *Coral Reefs: an ecosystem in transition*,
571 edited by: Dubinski, Z., and Stambler, N., Springer, 2011.

572 Fabricius, K., Langdon, C., Uthicke, S., Humphrey, C., Noonan, S., De'ath, G., Okazaki,
573 R., Muehllehner, N., Glas, M., and Lough, J.: Losers and winners in coral reefs
574 acclimatized to elevated carbon dioxide concentrations, *Nature Climate Change*, 1, 165-
575 169, 2011.

576 Fabricius, K. E.: Effects of terrestrial runoff on the ecology of corals and coral reefs:
577 review and synthesis, *Mar. Pollut. Bull.*, 50, 125-146, 2005.

578 Fair, R. C.: On the robust estimation of econometric models, in: *Annals of Economic and*
579 *Social Measurement*, Volume 3, number 4, NBER, 117-128, 1974.

580 Fang, J. K. H., Mello-Athayde, M. A., Schönberg, C. H. L., Kline, D. I., Hoegh-
581 Guldberg, O., and Dove, S.: Sponge biomass and bioerosion rates increase under ocean
582 warming and acidification, *Global Change Biology*, 19, 3581-3591, 2013.

583 Fanguie, N. A., O'Donnell, M. J., Sewell, M. A., Matson, P. G., MacPherson, A. C., and
584 Hofmann, G. E.: A laboratory-based, experimental system for the study of ocean
585 acidification effects on marine invertebrate larvae, *Limnology and Oceanography*:
586 *Methods*, 8, 441-452, 2010.

587 Feely, R. A., Sabine, C. L., Lee, K., Berelson, W., Kleypas, J., Fabry, V. J., and Millero,
588 F. J.: Impact of anthropogenic CO₂ on the CaCO₃ system in the oceans, *Science*, 305,
589 362-366, 2004.

- 590 Findlay, H. S., Wood, H. L., Kendall, M. A., Spicer, J. I., Twitchett, R. J., and
591 Widdicombe, S.: Comparing the impact of high CO₂ on calcium carbonate structures in
592 different marine organisms, *Marine Biology Research*, 7, 565-575, 2011.
- 593 Gattuso, J.-P., Frankignoulle, M., and Smith, S. V.: Measurement of community
594 metabolism and significance in the coral reef CO₂ source-sink debate, *Proceedings of the*
595 *National Academy of Sciences*, 96, 13017-13022, 1999.
- 596 Guadayol, Ò., Silbiger, N. J., Donahue, M. J., and Thomas, F. I. M.: Patterns in Temporal
597 Variability of Temperature, Oxygen and pH along an Environmental Gradient in a Coral
598 Reef, *PloS one*, 9, e85213, DOI:10.1371/journal.pone.0085213, 2014.
- 599 [Harrington, L., Fabricius, K., De'ath, G., Negri, A., Recognition and selection of](#)
600 [settlement substrata determine post-settlement survival in corals. *Ecology*, 84-3428-3437,](#)
601 [2004.](#)
- 602 Hoegh-Guldberg, O., Mumby, P. J., Hooten, A. J., Steneck, R. S., Greenfield, P., Gomez,
603 E., Harvell, C. D., Sale, P. F., Edwards, A. J., Caldeira, K., Knowlton, N., Eakin, C. M.,
604 Iglesias-Prieto, R., Muthiga, N., Bradbury, R. H., Dubi, A., and Hatziolos, M. E.: Coral
605 reefs under rapid climate change and ocean acidification, *Science*, 318, 1737-1742, 2007.
- 606 [Huey, R.B., Kingsolver, J.G. Evolution of thermal sensitivity of ectotherm performance.](#)
607 [Trends Ecol. Evol., 4,131-135, 1989](#)
- 608 [Hutchings, P.A., Biological destruction of coral reefs, *Coral Reefs*, 4, 239-252, 1986.](#)
- 609 Hoegh-Guldberg, O., and Bruno, J. F.: The impact of climate change on the world's
610 marine ecosystems, *Science*, 328, 1523-1528, 2010.
- 611 Hurd, C. L., Cornwall, C. E., Currie, K., Hepburn, C. D., McGraw, C. M., Hunter, K. A.,
612 and Boyd, P. W.: Metabolically induced pH fluctuations by some coastal calcifiers
613 exceed projected 22nd century ocean acidification: a mechanism for differential
614 susceptibility?, *Global Change Biology*, 17, 3254-3262, 2011.
- 615 Johnson, M. D., and Carpenter, R. C.: Ocean acidification and warming decrease
616 calcification in the crustose coralline alga *Hydrolithon onkodes* and increase
617 susceptibility to grazing, *J. Exp. Mar. Biol. Ecol.*, 434, 94-101, 2012.
- 618 Johnson, M. D., Moriarty, V. W., and Carpenter, R. C.: Acclimatization of the Crustose
619 Coralline Alga *Porolithon onkodes* to Variable pCO₂, *PLOS ONE*, 9, e87678, DOI:
620 10.1371/journal.pone.0087678, 2014.
- 621 Jokiel, P. L., Rodgers, K. S., Kuffner, I. B., Andersson, A. J., Cox, E. F., and Mackenzie,
622 F. T.: Ocean acidification and calcifying reef organisms: a mesocosm investigation, *Coral*
623 *Reefs*, 27, 473-483, 2008.
- 624 Jury, C. P., Thomas, F. I. M., Atkinson, M. J., and Toonen, R. J.: Buffer Capacity,
625 Ecosystem Feedbacks, and Seawater Chemistry under Global Change, *Water*, 5, 1303-
626 1325, 2013.
- 627 Kamenos, N. A., Burdett, H. L., Aloisio, E., Findlay, H. S., Martin, S., Longbone, C.,
628 Dunn, J., Widdicombe, S., and Calosi, P.: Coralline algal structure is more sensitive to

Formatted: Subscript

Formatted: Subscript

629 rate, rather than the magnitude, of ocean acidification, *Global Change Biology*, 19, 3621-
630 3628, 2013.

631 Kleypas, J., and Langdon, C.: Coral reefs and changing seawater chemistry, in: *Coral*
632 *Reefs and Climate Change: Science and Management.*, edited by: Phinney, J., Skirving,
633 W., Kleypas, J., and Hoegh-Guldberg, O., American Geophysical Union, Washington
634 D.C., pp. 73-110, 2006.

635 Kroeker, K. J., Kordas, R. L., Crim, R. N., and Singh, G. G.: Meta-analysis reveals
636 negative yet variable effects of ocean acidification on marine organisms, *Ecology Letters*,
637 13, 1419-1434, 2010.

638 Kroeker, K. J., Kordas, R. L., Crim, R., Hendriks, I. E., Ramajo, L., Singh, G. S., Duarte,
639 C. M., and Gattuso, J. P.: Impacts of ocean acidification on marine organisms:
640 quantifying sensitivities and interaction with warming, *Global Change Biology*, 19, 1884-
641 1896, 2013.

642 [Littler, M.M. The population and community structure of Hawaiian fringing-reef](#)
643 [crustose corallinaceae \(Rhodophyta, Cryptonemiales\), *Journal of Experimental Marine*](#)
644 [Biology and Ecology](#), 11, 103-120, 1973.

645 Lowe, R. J., Falter, J. L., Monismith, S. G., and Atkinson, M. J.: A numerical study of
646 circulation in a coastal reef-lagoon system, *Journal of Geophysical Research-Oceans*,
647 114, C06022, 2009a.

648 Lowe, R. J., Falter, J. L., Monismith, S. G., and Atkinson, M. J.: Wave-driven circulation
649 of a coastal reef-lagoon system, *J. Phys. Oceanogr.*, 39, 873-893, 2009b.

650 Martin, S., Cohu, S., Vignot, C., Zimmerman, G., and Gattuso, J. P.: One-year
651 experiment on the physiological response of the Mediterranean crustose coralline alga,
652 *Lithophyllum cabiochae*, to elevated pCO₂ and temperature, *Ecology and evolution*, DOI:
653 10.1029/2008JC005081, 2013.

654 Mehrbach, C.: Measurement of the apparent dissociation constants of carbonic acid in
655 seawater at atmospheric pressure, *Limnol. Oceanogr.*, 18, 897-907, 1973.

656 Meinshausen, M., Smith, S. J., Calvin, K., Daniel, J. S., Kainuma, M. L. T., Lamarque, J.
657 F., Matsumoto, K., Montzka, S. A., Raper, S. C. B., and Riahi, K.: The RCP greenhouse
658 gas concentrations and their extensions from 1765 to 2300, *Climatic Change*, 109, 213-
659 241, 2011.

660 Pandolfi, J. M., Connolly, S. R., Marshall, D. J., and Cohen, A. L.: Projecting coral reef
661 futures under global warming and ocean acidification, *Science*, 333, 418-422, 2011.

662 [Price, N., Habitat selection, facilitation, and biotic settlement cues affect distribution and](#)
663 [performance of coral recruits in French Polynesia, *Oecologia*](#), 163, 747-758, 2010.

664 [Pörtner, H.O., Bennet, A.F., Bozinovic, F., Clarke, A., Lardies, M.A., Lucassen, M.,](#)
665 [Pelster, B., Schiemer, F., Stillman, J.H., Trade-offs in therman adaptation: the need for](#)
666 [molecular ecological integration, *Phys. Biochem. Zool.*](#), 79, 295-313, 2006.

667 [Putnam, H.M. Resilience and acclimitization potential of reef corals under predicted](#)
668 [climate change stressors, PhD, Zoology, University of Hawaii at Manoa, Honolulu, 2012](#)

- 669 Reyes-Nivia, C., Diaz-Pulido, G., Kline, D., Guldberg, O.-H., and Dove, S.: Ocean
670 acidification and warming scenarios increase microbioerosion of coral skeletons, *Global*
671 *Change Biology*, 19, 1919-1929, 2013.
- 672 Ries, J. B., Cohen, A. L., and McCorkle, D. C.: Marine calcifiers exhibit mixed responses
673 to CO₂-induced ocean acidification, *Geology*, 37, 1131-1134, 2009.
- 674 Rodolfo-Metalpa, R., Houlbrèque, F., Tambutté, É., Boisson, F., Baggini, C., Patti, F. P.,
675 Jeffree, R., Fine, M., Foggo, A., and Gattuso, J. P.: Coral and mollusc resistance to ocean
676 acidification adversely affected by warming, *Nature Climate Change*, 1, 308-312, 2011.
- 677 Rogelj, J., Meinshausen, M., and Knutti, R.: Global warming under old and new
678 scenarios using IPCC climate sensitivity range estimates, *Nature Climate Change*, 2, 248-
679 253, 2012.
- 680 Sanford, T., Frumhoff, P. C., Luers, A., and Gullede, J.: The climate policy narrative for
681 a dangerously warming world, *Nature Climate Change*, 4, 164-166, 2014.
- 682 Semesi, I. S., Kangwe, J., and Björk, M.: Alterations in seawater pH and CO₂ affect
683 calcification and photosynthesis in the tropical coralline alga, *Hydrolithon*
684 sp.(Rhodophyta), *Estuarine, Coastal and Shelf Science*, 84, 337-341, 2009.
- 685 Silbiger, N., Guadayol, Ò., Thomas, F. I., and Donahue, M.: Reefs shift from net
686 accretion to net erosion along a natural environmental gradient, *Marine Ecology Progress*
687 *Series*, 515, 33-44, 2014.
- 688 Smith, S. V., and Key, G. S.: Carbon dioxide and metabolism in marine environments,
689 *Limnol. Oceanogr*, 20, 493-495, 1975.
- 690 Smith, S. V., Kimmerer, W. J., Laws, E. A., Brock, R. E., and Walsh, T. W.: Kaneohe
691 Bay sewage diversion experiment- perspectives on ecosystem responses to nutritional
692 perturbation, *Pacific Science*, 35, 279-402, 1981.
- 693 [Solomon, S., Qin, D., Manning, M., Chen, Z., Marquis, M., et al. Climate Change 2007:](#)
694 [The physical Science Basis: Contributions of Working Group I to the Fourth Assessment](#)
695 [Report of the Intergovernmental Panel on Climate Change., New York, Cambridge Univ.](#)
696 [Press, 2007.](#)
- 697 Stimson, J., and Kinzie III, R. A.: The temporal pattern and rate of release of
698 zooxanthellae from the reef coral *Pocillopora damicornis* (Linnaeus) under nitrogen-
699 enrichment and control conditions, *Journal of Experimental Marine Biology and Ecology*,
700 153, 63-74, 1991.
- 701 Tans, P., and Keeling, R.: NOAA/ESRL, www.esrl.noaa.gov/gmd/ccgg/trends/, 2013.
- 702 Tribollet, A., and Payri, C.: Bioerosion of the coralline alga *Hydrolithon onkodes* by
703 microborers in the coral reefs of Moorea, French Polynesia, *Oceanologica Acta*, 24, 329-
704 342, 2001.
- 705 Tribollet, A., Atkinson, M. J., and Langdon, C.: Effects of elevated pCO₂ on epilithic
706 and endolithic metabolism of reef carbonates, *Global Change Biology*, 12, 2200-2208,
707 2006.

- 708 | Tribollet, A., Godinot, C., Atkinson, M., and Langdon, C.: Effects of elevated $p\text{CO}_2$ on
709 dissolution of coral carbonates by microbial euendoliths, *Global Biogeochemical Cycles*,
710 23, GB3008, 2009.
- 711 Uppström, L. R.: The boron/chlorinity ratio of deep-sea water from the Pacific Ocean,
712 *Deep Sea Research and Oceanographic Abstracts*, 1974, 161-162.
- 713 Van Heuven, S., Pierrot, D., Lewis, E., and Wallace, D. W. R.: MATLAB Program
714 developed for CO₂ system calculations, Rep. ORNL/CDIAC-105b, 2009.
- 715 Van Vuuren, D. P., Meinshausen, M., Plattner, G. K., Joos, F., Strassmann, K. M., Smith,
716 S. J., Wigley, T. M. L., Raper, S. C. B., Riahi, K., and De La Chesnaye, F.: Temperature
717 increase of 21st century mitigation scenarios, *Proceedings of the National Academy of*
718 *Sciences*, 105, 15258-15262, 2008.
- 719 Van Vuuren, D. P., Edmonds, J., Kainuma, M., Riahi, K., Thomson, A., Hibbard, K.,
720 Hurtt, G. C., Kram, T., Krey, V., and Lamarque, J.-F.: The representative concentration
721 pathways: an overview, *Climatic Change*, 109, 5-31, 2011.
- 722 White, J.: Distribution, recruitment and development of the borer community in dead
723 coral on shallow Hawaiian reefs, Ph.D., Zoology, University of Hawaii at Manoa,
724 Honolulu, 1980.
- 725 Wisshak, M., Schönberg, C. H. L., Form, A., and Freiwald, A.: Ocean acidification
726 accelerates reef bioerosion, *Plos One*, 7, e45124-e45124, 2012.
- 727 Wisshak, M., Schönberg, C. H. L., Form, A., and Freiwald, A.: Effects of ocean
728 acidification and global warming on reef bioerosion—lessons from a clonoid sponge,
729 *Aquatic Biology*, 19, 111-127, 2013.
- 730 | [Wolf-Gladrow, D.A., Zeebe, R.E., Klass, C., Körtzinger, A., Dickson, A.G.: Total](#)
731 [Alkalinity: The explicit conservative expression and its application to biogeochemical](#)
732 [processes, *Marine Chemistry*, 106, 287-300, 2007.](#)
- 733 Yates, K. K., and Halley, R. B.: CO_3^{2-} concentration and $p\text{CO}_2$ thresholds for calcification
734 and dissolution on the Molokai reef flat, Hawaii, *Biogeosciences*, 3, 357-369, 2006.
- 735

736 Table 1: Means and standard errors of all measured parameters by rack. $p\text{CO}_2$, HCO_3^- , CO_3^{2-} , DIC, and Ω_{arag} were all calculated from
 737 the measured TA and pH samples using CO2SYS. Each table entry is the mean of 12 water samples: one daytime sample and one
 738 nighttime sample for six aquaria within a rack. Data are all from the imposed treatment conditions with no rubble inside the aquaria.

| Rack | Pre-industrial | Present Day | 2050 prediction | 2100 prediction |
|---|----------------|-----------------|-----------------|-----------------|
| Temp (°C) | 23.8±0.07 | 24.8±0.08 | 26.2±0.06 | 27.2±0.08 |
| Salinity(psu) | 35.65±0.01 | 35.71±0.02 | 35.62±0.02 | 35.71±0.02 |
| Total Alkalinity ($\mu\text{mol kg}^{-1}$) | 2137±1.7 | 2138±2.3 | 2139±2.0 | 2142±1.9 |
| pH _t | 8.02±0.02 | 7.87±0.01 | 7.74±0.02 | 7.67±0.02 |
| pCO ₂ (μatm) | 409±20.0 | 614±15.6 | 868±33.0 | 1047±38.7 |
| HCO ₃ ⁻ ($\mu\text{mol kg}^{-1}$) | 1692±16.9 | 1815±7.3 | 1894±7.8 | 1939±6.6 |
| CO ₃ ²⁻ ($\mu\text{mol kg}^{-1}$) | 194.20±6.7 | 147.08±2.8 | 113.98±3.8 | 99.24±3.3 |
| DIC ($\mu\text{mol kg}^{-1}$) | 1898±10.9 | 1980±5.1 | 2032±5.0 | 2067±4.5 |
| Ω_{arag} | 3.06±0.1 | 2.32±0.04 | 1.80±0.06 | 1.57±0.05 |
| NO ₂ ⁻ ($\mu\text{mol L}^{-1}$) | 0.082 ± 0.0028 | 0.078 ± 0.0045 | 0.074 ± 0.0047 | 0.070 ± 0.0051 |
| PO ₄ ³⁻ ($\mu\text{mol L}^{-1}$) | 0.017 ± 0.014 | 0.0097 ± 0.0081 | 0.033 ± 0.016 | 0.018±0.0061 |
| Si(OH) ₄ ($\mu\text{mol L}^{-1}$) | 3.60 ± 0.58 | 3.64 ± 0.61 | 3.88 ± 0.49 | 3.78 ± 0.52 |
| NH ₄ ⁺ ($\mu\text{mol L}^{-1}$) | 0.45 ± 0.30 | 0.19 ± 0.067 | 0.23 ± 0.15 | 0.34 ± 0.14 |
| NO ₃ ⁻ ($\mu\text{mol L}^{-1}$) | 2.13±0.20 | 2.25±0.21 | 2.55±0.10 | 2.48±0.11 |

739 Table 2: Regression results for the treatment experiments: G_{day} , G_{night} , and G_{net} versus
 740 Standardized Climate Change (Figure 3-3a,c,e) and NCP_{day} , NCP_{night} , and NCP_{net} versus
 741 Standardized Climate Change (Figure 3b,d,f). Bold values indicate a statistically significant
 742 p-value at an $\alpha < 0.05$.

| | SS | df | F | p | R ² |
|--|------------------------------|-----------|------------------|-------------------|--------------------------|
| G_{day} | | | | | |
| Standardized Climate Change | <u>5.823.79</u> | 1 | <u>1.9745</u> | <u>0.1706</u> | |
| (Standardized Climate Change) ² | <u>18.6723</u> | 1 | <u>6.33</u> | 0.02 | |
| Error | <u>61.86</u> | 21 | <u>2.95</u> | | <u>0.29</u> |
| G_{night} | | | | | |
| Standardized Climate Change | <u>73.6067</u> | 1 | <u>50.0939.1</u> | <0.0001 | |
| Error | <u>32.32</u> | 22 | | | <u>0.70</u> |
| G_{net} | | | | | |
| Standardized Climate Change | <u>89.7988</u> | 1 | <u>20.2519.4</u> | <0.001 | |
| Error | <u>97.57</u> <u>99.35</u> | 22 | <u>0.002</u> | | <u>0.48</u> <u>47</u> |
| NCP_{day} | | | | | |
| <u>Standardized Climate Change</u> | <u>5687.2</u> | <u>1</u> | <u>57.36</u> | <0.0001 | |
| <u>Error</u> | <u>2181.4</u> | <u>22</u> | | | <u>0.72</u> |
| NCP_{night} | | | | | |
| <u>Standardized Climate Change</u> | <u>3816.1</u> | <u>1</u> | <u>52.06</u> | <0.0001 | |
| <u>Error</u> | <u>1612.6</u> | <u>22</u> | | | <u>0.70</u> |
| NCP_{net} | | | | | |
| <u>Standardized Climate Change</u> | <u>17925</u> | <u>1</u> | <u>121.47</u> | <0.0001 | |
| <u>Error</u> | <u>3246.4</u> | <u>22</u> | | | <u>0.85</u> |

743

744

Formatted: Numbering: Continuous

Formatted: Left

Formatted: Left

Formatted: Left

Formatted Table

Formatted: Left

Formatted: Left

Formatted: No Spacing, Line spacing: single

Formatted: Left

Formatted: Left, Line spacing: 1.5 lines

Formatted: Justified

Formatted: Left

Formatted: Left

Formatted: Justified

Formatted: Left

Formatted: No Spacing, Line spacing: single

Formatted: Justified

Formatted: Left

Formatted: Justified

Formatted: Justified

Formatted: Left

Formatted: Left

Formatted: No Spacing, Line spacing: single

Formatted: Left

Formatted: Left

745 **Figure legends:**

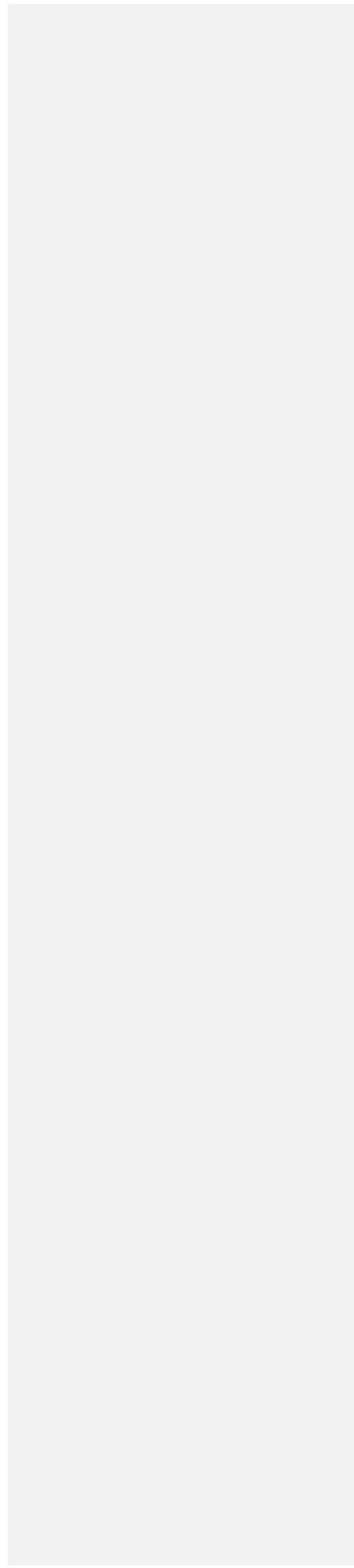
746 **Figure 1:** A schematic of the mesocosm system at the Hawai'i Institute of Marine Biology.
747 Ambient seawater is pumped into the system from a nearby fringing reef in Kāne'ōhe Bay.
748 The seawater is filtered with a sand trap filter, passed through a water chiller and then fed into
749 one of four header tanks. pCO₂ is manipulated in each header tank by bubbling a mixture of
750 CO₂-free air and pure CO₂ to the desired concentration. The water from one header tank flows
751 into 6 aquaria (a rack). Light is controlled by rack with metal-halide lights. There are two
752 metal-halide lights per rack with each light oscillating over a set of three aquaria. Flow and
753 temperature are controlled in each individual aquarium with flow valves and aquarium heaters
754 and coolers, respectively.

755 **Figure 2:** pCO₂ and temperature in each aquarium (a) without any rubble present and (b) with
756 rubble present. Daily variability in pCO₂ was higher when rubble was present due to
757 feedbacks from the rubble community (Notenote the different x-axis scales in panels a and b).
758 Panel (c) shows the mean difference between day and night pCO₂ with and without rubble
759 present with observations paired by aquarium (error bars are standard error) ($t_{23} = -7.23$,
760 $p < 0.0001$).

761 **Figure 3:** Net ecosystem calcification: (a) G_{day} , (b) G_{night} , (c) G_{net} and net community
762 production (d) NCP_{day} , (e) NCP_{night} , and (f) NCP_{net} versus Standardized Climate Change-
763 (SCC). Each point represents net ecosystem calcification (left panel) or net community
764 production (right panel) calculated from an individual aquarium. Standardized Climate
765 Change was centered around background seawater conditions such that a value of 0 indicated
766 that there was no change in pCO₂ or temperature. Positive values indicate an elevated pCO₂
767 and temperature condition relative to background and negative values represent lower pCO₂
768 and temperature conditions. G_{day} had a non-linear relationship with Standardized Climate

769 Change ($y = -1.6 \times 10^{-8} 0.27 x^2 + 1.4 \times 10^{-4} 0.59x + 5.57$), while G_{night} ($y = -1.0.63x - 3 \times 10^{-4} x -$
770 $3.4.6$) and G_{net} ($y = -0.76x + 1.7 \times 10^{-4} x + 1.4$) each had a negative linear relationship with
771 Standardized Climate Change (Table 2). NCP_{day} ($y = -7.01x + 23.4$), NCP_{night} ($y = -35.76 - 4.74$),
772 and NCP_{net} ($y = -12.07x - 10.85$) all had significant negative relationships with Standardized
773 Climate Change. Black lines are best fit lines for each model with 95% confidence intervals in
774 gray. Greek letters on the top panel represent the imposed conditions for pre-industrial (α),
775 Present Day (β), 2050 (γ), and 2100 (δ). The black horizontal line in in panels (b), (e) and (f)
776 shows the point where G and NCP = 0. Points above the line are net calcifying (e) or net
777 photosynthesizing (f) and points below the line are net dissolving (e) or net respiring (f) over
778 the entire 24 hour period.

779 **Figure 4:** (a) Calculated G and NCP rates for all treatment aquaria. The color represents
780 Standardized Climate Change. Squares are data collected during the light (day) conditions and
781 circles represent data collected during dark (night) conditions. All negative numbers are either
782 net dissolution or net respiration while positive numbers are net calcification or net
783 photosynthesis, and the color represents Standardized Climate Change (color bar). There is a
784 strong positive relationship between G and NCP ($y = 0.14x + 1.9$, $p < 0.0001$, $R^2 = 0.85$).
785 Negative and positive y-values are net dissolution and net calcification, respectively; negative
786 and positive x-values are net respiration and net photosynthesis, respectively. (b) TA versus
787 DIC: There is a strong positive relationship between TA and DIC ($y = 0.31x + 1577.4$,
788 $p < 0.0001$, $R^2 = 0.85$). Black and gray lines represent the best-fit line and 95% confidence
789 intervals, respectively. Supplementary Figure A3 is a similar plot with specific aquaria
790 labeled. As expected, the slope of TA versus DIC (0.31) is approximately twice that of G
791 versus NCP (0.14).



793 **Appendix A:**
 794 **Supplemental Material:**
 795 **Tables A1-A2**
 796 **Figures A1-A46**

797 Table A1: Analysis of ~~treatment experiment using ANOVA table (Figure A4)~~ variance for
 798 G_{day} , G_{night} , and G_{net} versus ~~Standardized Climate Change~~. Bold values indicate a statistically
 799 significant p value at an $\alpha < 0.05$ across the four climate scenario treatments (Figure A3).

800

| | SS | df | MS | F | p | Formatted Table |
|--------------------------------------|--------|----|-------|------|-------------------|-----------------|
| G_{day} | | | | | | |
| <u>Treatment</u> Groups | 28.83 | 3 | 9.81 | 3.65 | 0.030 | Formatted Table |
| Error | 52.61 | 20 | 2.63 | | | |
| Total | 81.45 | 23 | | | | |
| G_{night} | | | | | | |
| Groups | 60.39 | 3 | 20.13 | 8.84 | <0.0001 | Formatted Table |
| Error | 45.53 | 20 | 2.28 | | | |
| Total | 105.92 | 23 | | | | |
| G_{net} | | | | | | |
| Groups | 104.31 | 3 | 34.77 | 8.37 | <0.0001 | Formatted Table |
| Error | 83.05 | 20 | 4.15 | | | |
| Total | 197.36 | 23 | | | | |

801

802

803 Table A2: Analysis of variance for NCP_{day}, NCP_{night}, and NCP_{net} versus climate scenario
 804 treatments (Figure A4).Climate Change.

| | <u>SS</u> | <u>df</u> | <u>MS</u> | <u>F</u> | <u>p</u> |
|-----------------------------------|---------------|-----------|---------------|-------------|--------------------------|
| <u>NCP_{day}</u> | | | | | |
| <u>Treatment</u> | <u>6265.3</u> | <u>3</u> | <u>2088.4</u> | <u>26.0</u> | <u><0.0001</u> |
| <u>Error</u> | <u>1603.2</u> | <u>20</u> | <u>80.2</u> | | |
| <u>Total</u> | <u>7868.6</u> | <u>23</u> | | | |
| <u>NCP_{night}</u> | | | | | |
| <u>Treatment</u> | <u>4145.2</u> | <u>3</u> | <u>1381.7</u> | <u>21.5</u> | <u><0.0001</u> |
| <u>Error</u> | <u>1283.4</u> | <u>20</u> | <u>64.2</u> | | |
| <u>Total</u> | <u>5428.6</u> | <u>23</u> | | | |
| <u>NCP_{net}</u> | | | | | |
| <u>Treatment</u> | <u>1936.8</u> | <u>3</u> | <u>6456.0</u> | <u>71.6</u> | <u><0.0001</u> |
| <u>Error</u> | <u>1803.4</u> | <u>20</u> | <u>90.17</u> | | |
| <u>Total</u> | <u>2117.1</u> | <u>23</u> | | | |

805
 806
 807
 808 **Figure A1:** Feedbacks in seawater chemistry caused by the presence of rubble during the (a)
 809 day and (b) night. X-axis is pCO₂ in seawater without any rubble and y-axis is pCO₂ in
 810 seawater with rubble present. Color represents temperature. ~~The top panel is data collected~~
 811 ~~during the day and the bottom panel is data collected at night.~~The black dashed line is a 1:1
 812 line- and the blue line is a regression line. The pCO₂ conditions drift farther away from the
 813 manipulated conditions during the night. The slopes from each regression analysis were both
 814 greater than one (Day: $y = 1.12x + 19.83$, Night: $y = 1.43x + 44.54$) meaning that the

815 biological feedbacks were greater at more extreme treatments and greater during the night
816 than the day.

817 **Figure A2:** Boxplots for G_{day} (Aa), G_{night} (Bb), and G_{net} (Cc) for the control experiment,
818 separated by rack. We used an ANOVA to test for differences across racks and found no
819 significant difference in G_{day} ($F_{3,23}=0.68$, $p=0.58$), G_{night} ($F_{3,23}=1.52$, $p=0.24$), or G_{net}
820 ($F_{3,23}=1.38$, $p=0.28$).

821 **Figure A3:** ~~Panel A is G versus NCP rates numbered by tank. Data and best fit line are the~~
822 ~~same as Figure 4. Panel B is salinity normalized TA on the y axis and salinity normalized~~
823 ~~DIC on the x axis in $\mu\text{mol kg}^{-1}$. There is a strong positive relationship between TA and DIC (y~~
824 ~~$= 0.31x + 0.0016$, $p < 0.0001$, $R^2 = 0.85$).~~

825 **Figure A4:** Means and standard error bars for (a) G_{day} , (b) G_{night} , and (c) G_{net} in $\text{mmol m}^{-2} \text{d}^{-1}$.
826 ~~X axis represents in the four~~ climate scenario ~~treatments.treatment categories~~. There were
827 significant differences ~~aerossbetween~~ treatments for G_{day} ($p=0.03$), G_{night} ($p < 0.0001$), and G_{net}
828 ($p < 0.0001$) (Table A1).

829

830

831

832

833 **Figure A4:** Means and standard error bars for (a) NCP_{day} , (b) $\text{NCP}_{\text{night}}$, and (c) NCP_{net} in
834 $\text{mmol m}^{-2} \text{d}^{-1}$ across the four climate scenario treatments. There were significant differences
835 across treatments for NCP_{day} ($p < 0.0001$), $\text{NCP}_{\text{night}}$ ($p < 0.0001$), and NCP_{net} ($p < 0.0001$) (Table
836 A2).

837 **Figure A5:** Net ecosystem calcification (G_{day} , G_{night} , and G_{net}) versus Δ Temperature (left
 838 panel) and ΔpCO_2 (right panel). Lines are best fit lines. G_{day} has a significant non-linear
 839 relationship ΔpCO_2 ($p=0.04$) and Δ Temperature ($p=0.01$). G_{night} , (Δ Temp: $p<0.001$, ΔpCO_2 :
 840 $p<0.001$) and G_{net} (Δ Temp: $p<0.001$, ΔpCO_2 : $p<0.001$) both have significant linear
 841 relationships with ΔpCO_2 and Δ Temperature.

842 **Figure A6:** Net community production (NCP_{day} , NCP_{night} , and NCP_{net}) versus Δ Temperature
 843 (left panel) and ΔpCO_2 (right panel). Lines are best fit lines. NCP_{day} (Δ Temp: $p<0.001$,
 844 ΔpCO_2 : $p<0.001$), NCP_{night} , (Δ Temp: $p<0.001$, ΔpCO_2 : $p<0.001$) and NCP_{net} (Δ Temp:
 845 $p<0.001$, ΔpCO_2 : $p<0.001$) all have significant linear relationships with ΔpCO_2 and
 846 Δ Temperature.

847 **G and NCP calculations:** Below are the specific calculations for G and NCP for Equations 1
 848 and 2 in the text (in $mmol\ C\ m^{-2}\ hr^{-1}$). For comparisons with existing literature, G and NCP
 849 were both multiplied by 12 hr/day to get $mmol\ m^{-2}\ d^{-1}$.

850 Equation 1 (equations modified from Andersson et al. 2009):

851 _____
 852
$$G = [F_{TAin} - F_{TAout} - \frac{dTA}{dt}] / 2$$
 _____ (A1)

853 F_{TAin} is the rate of TA flowing into the aquaria in $mmol\ CaCO_3\ m^{-2}\ hr^{-1}$:

854 _____
 855
$$F_{TAin} = ((TA_{H,t2} + TA_{H,t1}) \frac{1}{2} * FlowRate_{aq}) / 1000$$
 _____ (A2)

856 F_{TAout} is the rate of TA flowing out of the aquaria in $mmol\ CaCO_3\ m^{-2}\ hr^{-1}$:

857 _____
 858
$$F_{TAout} = ((TA_{aq,t2} + TA_{aq,t1}) \frac{1}{2} * FlowRate_{aq}) / 1000$$
 _____ (A3)

859 $\frac{dTA}{dt}$ is the change in TA in each aquaria in $mmol\ CaCO_3\ m^{-2}\ hr^{-1}$:

860

$$\frac{dTA}{dt} = \frac{TA_{aq,t2} - TA_{aq,t1} + Vol * \rho}{\Delta t * SA} \quad (A4)$$

862 Each equation is divided by 1000 to convert from μmol of CaCO_3 to mmol of CaCO_3

863 Parameters:

864 $TA_{H,t1}$ = Total alkalinity in the header tank at the first sampling time point ($\mu\text{Eq kg}^{-1}$).

865 $TA_{H,t2}$ = Total alkalinity in the header tank at the second sampling time point ($\mu\text{Eq kg}^{-1}$).

866 $TA_{aq,t1}$ = Total alkalinity in the aquarium at the first sampling time point ($\mu\text{Eq kg}^{-1}$).

867 $TA_{aq,t2}$ = Total alkalinity in the aquarium at the second sampling time point ($\mu\text{Eq kg}^{-1}$).

868 Δt = time between first and second sampling time point (h)

869 SA = surface area of the rubble in the aquarium (m^2)

870 Vol = volume of water in the aquarium (L)

871 ρ = density of seawater (kg L^{-1})

872 $FlowRate_{aq}$ = Flow rate of the water coming into the aquarium in $\text{kg m}^{-2} \text{h}^{-1}$ (equal to flow rate
873 of the water leaving the aquarium)

874

875 NCP is net community production rate in $\text{mmol C m}^{-2} \text{d}^{-1}$:

$$NCP = \left[F_{DICin} - F_{DICout} - \frac{dDIC}{dt} \right] - G \quad (A5)$$

877 F_{DICin} , F_{DICout} , $\frac{dDIC}{dt}$ are calculated in the same way as F_{TAin} , F_{TAout} , and $\frac{dTA}{dt}$ in Equations

878 A2-A4), replacing Total Alkalinity with Dissolved Inorganic Carbon.

Formatted: Subscript